



**VERTICAL LOADING ON SUCTION
CAISSON FOUNDATION**

MASTER'S THESIS

**ELIA MANZOTTI
2014**

THIS REPORT COLLECTS THE TWO ARTICLES "LABORATORY SETUP FOR VERTICALLY LOADED SUCTION CAISSON FOUNDATION IN SAND AND VALIDATION OF RESPONSES" AND "PRESENT KNOWLEDGE ABOUT LABORATORY TESTING OF AXIAL LOADING ON SUCTION CAISSONS", PRESENTED FOR M.SC. IN CIVIL AND STRUCTURAL ENGINEERING LONG MASTER'S THESIS AT AALBORG UNIVERSITY.

DEPARTMENT OF CIVIL ENGINEERING
AALBORG UNIVERSITY
SOHNGÅRDHOLMSVEJ 57
9000 AALBORG
WWW.SES.AAU.DK

Master's Thesis

Title:

Vertical Loading on Suction Caisson Foundation

Written by:

Elia Manzotti

M.Sc. Structural and Civil Engineering
School of Engineering and Science
Aalborg University

Supervisors:

Lars Bo Ibsen
Evelina Vaitkunaite

Project Period: 2013.09.01 – 2014.06.10

Elia Manzotti



DEPARTMENT OF CIVIL ENGINEERING
AALBORG UNIVERSITY

Synopsis

This paper collects two articles presented for long Master's Thesis project in Structural and Civil Engineering.

In the article "Laboratory Setup for Vertically Loaded Suction Caisson Foundation in Sand and validation of Responses", testing rig and procedure to carry out test at Aalborg University are presented. Then CPT-based method and beta methods are implemented. Parameters on which methods are based are analysed and fitted.

The article "Present Knowledge about Laboratory Testing of Axial Loading on Suction Caissons" is a state of the art, outcome of research on published literature regarding the topic.

The content of the report is freely available, though publication is only allowed with agreement of the authors.

Front-page picture is from <http://www.greenstyle.it/>.

Contents

Synopsis

Present knowledge about Laboratory Testing of Axial Loading on Suction Caissons.....	1
Laboratory Setup for Vertically loaded Suction Caisson Foundation in Sand and Validation of Responses.....	17
Digital Appendix.....	35

Present knowledge about Laboratory Testing of Axial Loading on Suction Caissons

Aalborg University, Department of Civil Engineering, Denmark.

Abstract: Offshore wind turbines are increasing in both efficiency and size. More economical foundations for such light structures are under investigation, and suction caisson was shown to be particularly suitable for this purpose. In multi-pod foundation configuration, the overturning moment given by loads on the structure is resisted by push-pull loads on the vertical axis of each suction caisson. Relevant works where this situation is examined by means of laboratory testing, are summarized in this article, then different conclusions are followed by discussion and comparison. In the initial theoretical section, an overview of phenomena related with the case of study is presented. Drained and undrained condition, liquefaction and suction are examined from the theoretical point of view for mechanisms related to the case of study.

1. INTRODUCTION

Wind turbines are usually founded on piles, these foundations are of simple design but take about 30% of the total budget. Suction caisson foundations are an option that can decrease the overall cost and increase the diffusion of wind turbine. Since wind turbine are dynamically sensitive structures where stiffness requirements have to be satisfied, an alternative design allowing to increase stiffness is multi-pod configuration (*Byrne 2002*), wherein loading response changes significantly with respect to a monopod. The following work is focused on loading of multi-pod foundation, where very little moment is taken by the suction caisson and the moment load is mainly resisted by push-pull load on the vertical axis of opposite suction caisson. For these reasons, it is important to understand behavior under tensile loading and improve the stiffness of foundation, so a correct design can be established. Among others, multi-pod foundations can be both tripod or tetrapod. Tripod has the advantage that it requires less material and it is easier to construct and install.

This review has the purpose to analyze research on vertical loading of suction caisson installed in sand, focusing on works done in laboratory. Cyclic and monotonic pull-out tests are reported, specifying equipment used and test modality adopted in order to discuss and compare works of different authors. It is recognized that the design of a wind turbine foundation is not driven by the ultimate capacity but it is governed by parameters as stiffness and behavior under cyclic loading, so particular attention has been given to these topics. Important matter is the enhancement in resistance to pull-out load given by pore pressure under the lid of the caisson. This resistance is a consequence of a complex interaction between permeability of the soil, drainage path and rate of loading, and is a resource on which can possibly contribute to peak load resistance. However a study needs to be done to have a more precise model of this phenomenon.

2. THEORETICAL OVERVIEW.

2.1 Laboratory Testing

Laboratory testing is a fundamental step of the assessment of the design procedure, inasmuch allow to test in a controlled environment phenomena of interest, and on which will be based the prototype design. Several types of laboratory setups were designed in order to test offshore foundations. Most of them examine the behavior of models which are about 100 times smaller than the full-scale foundations. Among the best known, are 1g and centrifuge tests which will be compared in this section.

In 1g models body forces cannot be modelled with a scale factor of one, friction angle is higher than the one in real size and Young modulus is lower. Since load-displacement response of sand depends also on void ratio, real condition can be reproduced in a scaled model reducing the density of the sand (*Randolph 2011*).

Centrifuge testing allows body forces to be modelled properly. In non-centrifuge small scale tests, stress-dependent behavior is modelled at low value of body forces, at which soil can show a different behavior and measurements have to be really accurate in order to get reliable results. Effective stress level in a centrifuge test is equal to the one of the prototype, strength ratio (shear strength over effective vertical stress) and stiffness ratio are scaled with a factor of 1 (*Mangal 1999*).

Drawback of centrifuge testing is the time scaling factors, that are $\frac{1}{N}$ and $\frac{1}{N^2}$ respectively for dynamic and seepage timing, where N is the acceleration level. To overcome this problem permeability of the soil has to be decreased, by increasing the viscosity or changing the grain size. Darcy describes the velocity for a laminar flow as $v = ki$ where the permeability is given by $k = K \frac{\gamma_w}{\mu}$ where γ_w represent the soil unit weight and μ the dynamic fluid viscosity. Since γ_w

increases linearly with the g level, μ has to be increased in order to reduce the permeability and keep the fluid velocity proportional to the prototype, therefore silicon oil is usually used in order to properly simulate the fluid flow through the soil

The capacity of centrifuges is given in g -tons, calculated as the multiplication of the maximum acceleration for the maximum package mass that fits in the centrifuge. The acceleration level is chosen in proportion to the depth that has to be modelled, dividing the height of the prototype for the height of the model.

Scaling relationship for 1 g and centrifuge tests is schematized in the following image, showing that in the centrifuge test body forces are scaled with a factor of 1 and distance is inversely proportional to the scaling factor.

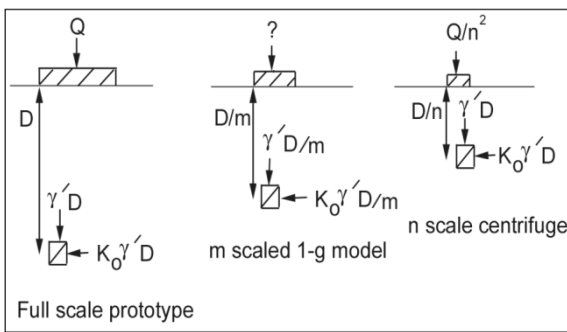


Figure 1. Scaling relationships for 1- g and centrifuge models (Murff 1996).

2.1 Drained and Undrained Condition

According to effective stress principle, after the application of a load, the drained condition occurs when the change in effective stress is equal to the change in total stress while the undrained condition occurs when the change in effective stress is equal to the difference between total stress and pore pressure. The intermediate state, partially drained conditions, occurs when the rate of volume change is greater than the flow rate of the fluid between the voids. Hence a variation of effective stress can be observed during the period of load application.

In a wind turbine foundation, various conditions can occur, depending on the soil permeability, the drainage length, and the rate of loading. When a suction caisson is installed in soil with low hydraulic conductivity is pulled out at high rate of loading, the trapped soil has an undrained behavior. In this case, theoretically, pore pressure developed below the lid corresponds to the applied pressure (tensile load divided by the area of the lid) and is limited by cavitation. Therefore the uplift resistance is given by the self-weight of the caisson plus external skirt friction and the weight of the soil plug trapped inside the caisson. Drained behavior, instead, is generated by high sand permeability and low rate of loading. In drained condition, uplift resistance is given by the self-

weight of the suction caisson, plus internal and external skirt friction. In undrained condition, the uplift resistance is generally greater than in drained condition.

In dense sand the expected behavior is of partially drained condition. Thus suction can occur below the lid, which increases the resistance capacity. The degree to which sand has a partially drained behavior, depends on the geometry of the caisson, the rate of loading, and drainage and deformation characteristics of the soil.

2.2 Liquefaction

In saturated sand, cyclic loading at relatively high frequencies can bring to an undrained behavior where pore water supports the load causing a decrease of effective stress. If the cyclic loading is rapid enough to not allow complete dissipation of pore water pressure, the latter can cause the effective stress going to zero and bringing the sand to a liquid state with low shear strength. This is the condition of soil liquefaction wherein sand has characteristics similar to those of a liquid. Even if effective stress is not zero, failure can occur because of the reduction in shear strength.

Liquefaction can often occur in loose sand, where cyclic loading creates a contractant behavior of the soil, causing a decrease in volume and an increase in pore pressure that cannot dissipate in undrained conditions. Generally, high void ratio and low confining pressure brings to a more rapid liquefaction. Time required for liquefaction is inversely proportional to the strain caused by cyclic loading, so the more strain is developed during each cycle, the less cycles are required to bring soil in a state of liquefaction.

During installation with suction, an upward flow of fluid is generated, and as a consequence an upward hydraulic gradient is formed inside the caisson. If difference in pressure is high, upward forces can exceed downward forces reducing to zero effective stresses, resulting in a liquefaction of the soil. This condition occurs when the critical hydraulic gradient is reached or exceeded. Critical gradient “ i ” is defined as the ratio between the effective unit soil weight and the unit weight of water $i = \gamma'_s / \gamma_w$ (Roy 2010).

2.3 Suction

On the studied cases, differentiation has to be made between active suction and passive suction. To install the suction caisson, active suction is created by means of pumps, and cannot be increased once the pump is disconnected. Passive suction is built up under the lid of the suction caisson as a consequence of upward displacement caused by loading.

Active suction during installation in sand establishes a flow in the soil surrounding the caisson. This flow reduces the vertical effective stresses of the skirt tip and on the interior of the caisson. Development of the upward hydraulic gradient inside the skirt reduces the side shear between soil and steel, while the downward flow of water outside the skirt increases the side shear, facilitating the penetration.

In model testing, a gradient close to the critical gradient is required to permit suction installation. This reduces the penetration resistance but, if it is not correctly evaluated, piping failure can occur preventing a complete penetration. This phenomena in field installation is avoided to some extent using water jetting or dredging pumps.

Installation in laboratory can be done also by pushing. It requires less equipment and do not give problems of active suction installation, such as liquefaction and creation of sand heave below the lid. The latter phenomenon occurs if the penetration resistance is not in equilibrium with active suction pressure, causing a deformation of the soil skeleton of which mechanism is not fully understood, and can cause a not complete installation of the model suction caisson with consequence on the test response (Tran 2005).

During tensile loading passive suction is creating a gradient in the same direction of the one of installation but, since the displacement is upwards, the gradient is acting in favor of resistance on the skirt friction. In drained to partially drained condition, the pressure gradient created between the lid and the bottom of the caisson creates a fully developed seepage flow from outside to inside the caisson. As consequence, the internal skirt friction is lower than the external one because internal effective stresses are reduced by the upward gradient, while external effective stresses are increased by the downward flow. In partially drained to undrained condition, the soil plug remains trapped within the caisson. Dilation occurs on the internal side of the skirt and in the area beneath the caisson, causing negative pore pressure and therefore a downward seepage also inside the caisson. As result, the uplift capacity increases due to the enhancement given by frictional resistance also on the inside of the skirt.

Enhancement of negative pore pressure is given also by dilatancy. If soil is in undrained condition, dilatancy can be fully developed, increasing resistance. This is not the case in most of the loading condition in dense sand, where there is a partially drained behavior instead. Therefore in partially drained condition, dilatancy has a reduced effect on pore pressure, since drainage results in volume deformation. From this consideration is it possible to infer that passive suction is inversely proportional to the degree of drainage and directly proportional to the rate of loading.

3. STATE OF THE ART.

3.1 Investigations of Suction Caissons in Dense Sand (Byrne 2000).

Equipment features

In this work a three degree of freedom loading rig was initially developed to test footings on clay (Martin 1994). At a later stage it was modified in order to cope with greater stiffness and displacement rates required for tests in sand (Mangal 1999). Load or displacement were applied by a

computer controlled stepper motor and measured with high accuracy ($\pm 2\text{N}$, $\pm 2\mu\text{m}$). Figure 2 shows the loading rig, details are given in Martin 1994, Gottardi and Houlsby (1995), Mangal (1999) and Byrne (1999).

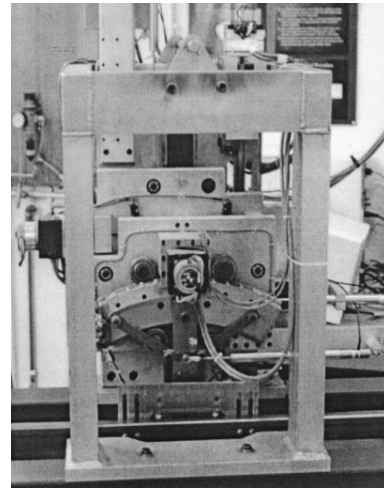


Figure 2. Loading rig (Byrne 2000).

Different loading programs were tested, tensile behavior was investigated in oil saturated sand samples, so in the following only these vertical load cases are discussed.

A tank of 1100 mm diameter and 350 mm depth was used to test dry and oil-saturated dense sand. This diameter has been considered large enough to allow performing multiple tests on the same sample of sand. Several testing of vertical loading behavior were made and are summarized in Table 4.1 and Table 4.5 in Byrne(1999), respectively for cyclic and monotonic tests. All tests were carried out with a suction caisson model with a diameter of 150mm and skirt length of 50mm (aspect ratio = 0.33). Pore pressure was measured with one pressure transducer positioned at the center below the lid, and two on the perimeter of the caisson.

Tests have been made in oil saturated samples of Baskarp Cyclone sand (Byrne 1999 Table 2.3), and prepared with a systematic procedure (Byrne 1999). A vacuum was applied at the top of loose sand before to vibrate it, so that full saturation was reached. Then alternating downward gradient and vibration, the wanted density was reached. Density in a range of 80-95% was estimated from CPT test by empirical formula from Mangal (1999), and drainage properties were evaluated with consolidation tests. Suction caisson model was installed at a speed of 0.05mm/s, keeping the valve on the top open so no piping failure occurs. Once a preload of 75N has been reached the valve were closed and the sample unloaded to 0N.

Sand samples were not prepared for each test and more tests were carried out on the same sample instead, every time loading with greater mean vertical load and then starting the test. For example in a typical cyclic test the footing was loaded with a sequence as: $100 \pm 25\text{N}$, $100 \pm 50\text{N}$, ..., $100 \pm 250\text{N}$. This means that for most of the test the soil was on the

elastic region, and only at the beginning of the sequence it reached the virgin curve. This represents the real physical situation, where extreme events are causing a small plastic deformation and then the loading remains in the elastic region.

Cyclic tests

In cyclic tests, a cyclic load was applied with “Constrained New Wave” method (Taylor et al., 1995) that ensures extreme events to be included in the random simulation. 100 cycles with 4 extreme events were applied at each test. Comparing tests where three different loading programs were applied, respectively “Constrained New Wave”, modulated sine wave, and stepped sine wave, it can be seen that there is no substantial difference in results. Despite that, “Constrained New Wave” method was used in most of the tests, because it reproduced the actual physical loading on the foundation.

Large number of tests were carried out, in Table 4.2, Table 4.3, and Table 4.4 in Byrne(1999) these tests are subdivided by relevance to the study of, respectively, frequencies, loading history and cyclic load ratio. Typical cyclic response is asymmetric, showing vertical load mobilized at greater displacement in tension with respect to compression. The load-displacement response changes gradually to an asymmetric response as the load moves closer to tension, see Figure 3.

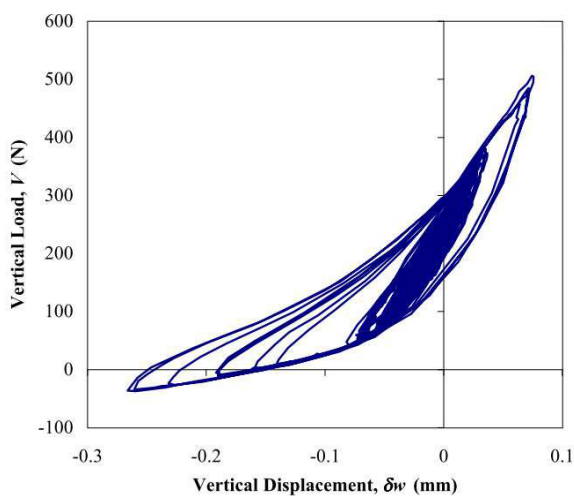


Figure 3. Asymmetrical cyclic response (Byrne 2000).

The range of period tested were from 1s to 30s and in all cases the response did not show any relevant change in behavior. Pore fluid response was relevant in both short and long period test. Longer periods were allowing the control system to have a better control on the loading and measuring devices, which in turn were allowing to reach a greater tensile displacement. In the long period test 1 mm displacement was mobilized at 200N, a displacement that was not reached in tests with faster period.

Monotonic pull-out test

Monotonic tests were carried out prescribing displacement and velocity. Tests were made for small and large displacements.

Effect of loading rate was analyzed applying small displacement, varying the rate of pull-out. A displacement of 1mm was applied at five different pull-out speed from 0.00086mm/s to 5mm/s in a sand sample with a relative density of 79%. The tensile capacity calculated was around 15N. This value is significantly lower than laboratory responses, meaning that, at small displacement, there was a partially drained behavior for all loading rates. In every test, most of the load was carried by pore fluid as shown in Figure 4 and there was a little variation of pressure applying different load rates.

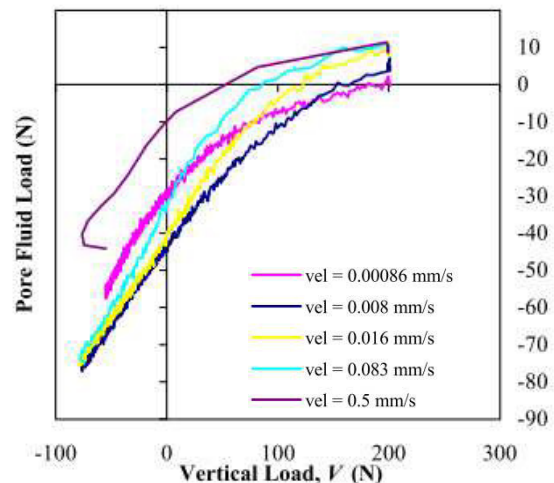


Figure 4. Pore pressure development (Byrne 2000).

Tests at small upward displacement with different loading history were carried out. Repeated pull-out tests on the same sample were showing a gradual decrease of the response, due to the loosening of the sample. An increment of tensile capacity was noticed after that a loading history causing re-densification of the soil was applied.

Pull-out tests in loose sand were showing a softening response in the initial stage of loading, followed by a stiffer response. To analyze this softening behavior, small and large displacement tests were carried out in a soil with a density of 94%, with the 150mm caisson, at different rates. Applying repeatedly small displacement (1mm) on the same sample, no degradation of response and no rate dependency appeared. It was noticed that the behavior was partially drained also for low rates of loading. For this reason, the a response was significantly higher than the drained capacity, since partially drained behavior allowed also at the pore pressure to carry the load. Remaining within serviceability requirements, greater displacements were applied repeatedly, and the response is showing a progressive degradation till the drained capacity is mobilized (weight of the soil plugged into the caisson plus contribution from external friction).

Large displacement tests were carried out with constant pull-out speed of 2mm/s. The initial softening behavior was studied applying small displacement, where a response independent from the rate of loading was noticed. As larger displacements were applied, within the limit of softening

behavior, the response become rate-dependent showing greater stiffness for high pull-out rates. When total pull-out was reached, after the softening response it was noticed a rate-dependent stiffer response, associated with dilation due to shear. In this latter response the stiffness was controlled by the velocity at which the water moved within the soil matrix to equilibrate the pressure difference created by the volume change that was occurring. The ultimate capacity was mobilized at large displacements, and was limited by cavitation. For this reason was suggested to design the tensile capacity on the initial softening response (Byrne 2000).

As can be seen in *Figure 5*, the total load response was greater than the pore fluid response. This gap is due to external friction, enhanced by a downward hydraulic gradient.

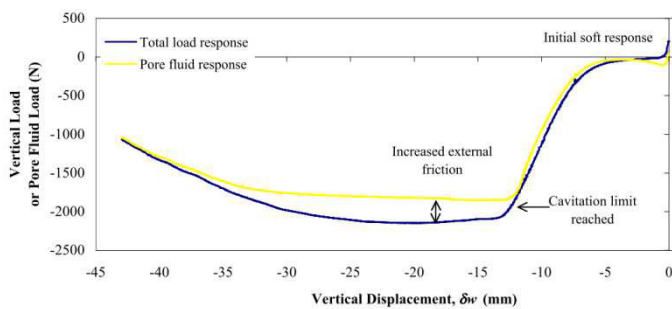


Figure 5. Response of high displacement pull-out (Kelly 2003).

Skirt effect was also analyzed, comparing pull-out tests of two footings with 100mm diameter and aspect ratio of 0 and 0.16. Tests were carried out at velocity of 2mm/s and the footing was preloaded with 100N load. Despite the small skirt, there was a great improvement of tension capacity due to the longer drainage path, and cavitation limit was reached using the 0.16 aspect ratio caisson.

3.2 Pressure Chamber Testing of Model Caisson Foundations in Sand (Kelly 2003).

Equipment features

Tests were carried out in a cylindrical pressure chamber (*Figure 6*), 1m diameter and 1m high, designed to develop a maximum pressure of 200kPa. Loads or displacements were applied by a hydraulic actuator, installed on the lid of the pressure chamber. The actuator had a capacity of 100kN and a maximum rate of load-controlled cycling frequency of 10 Hz.

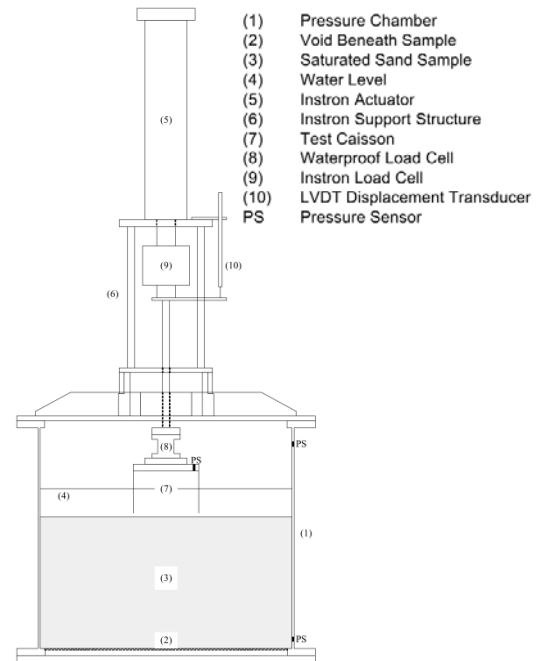


Figure 6. Pressure chamber (Kelly 2003).

A 100kN capacity load cell was used to measure the load. Displacements were measured by a system of Linear Variable Differential Transformer (LVDT). Two pressure transducers were installed in the pressure chamber. One was fitted at the top and the other at the bottom, so comparison could be made and hydraulic gradient could be measured. On the model caisson the pressure was measured by two pressure transducers, installed beneath the lid and at the tip of the skirt.

Model caisson was made of aluminum, it had a diameter of 280mm and a skirt length of 180mm (aspect ratio of 0.64). Caisson's skirt had a thickness of 3mm and the lid was 28mm thick. A vent valve was installed on the lid, in order to prevent water pressure building up during installation phase.

Tests were carried out with sand Redhill 110, sieve test results are shown in *Kelly (2006)*. The sand was vibrated in order to reach a $D_r=80\%$. Sample preparation process is reported in *Kelly et al. (2003)*.

Testing

The caisson was installed with a velocity of 0.2mm/s, till a compression load of 30kN. Tests were carried out at a frequency of 1Hz. 10 cycles were applied with amplitudes of $\pm 5\text{kN}$, $\pm 10\text{kN}$, $\pm 20\text{kN}$, $\pm 30\text{kN}$, then 5 cycles were applied with amplitudes of $\pm 35\text{kN}$ and $\pm 40\text{kN}$. In between of each set of cycles the pore pressure was allowed to dissipate. After the last set of cycles a pull-out test was carried out at a rate of 5mm/s. Due to the rate of loading and permeability property of the sand, the behavior of the soil was drained to partially drained.

During the cyclic tests, low tensile loads were reached: on the $\pm 40\text{kN}$ amplitude set of cycle, only -1kN was mobilized on a

target of -5kN. As the load goes into tension there was a dropping of stiffness as can be seen from *Figure 7*.

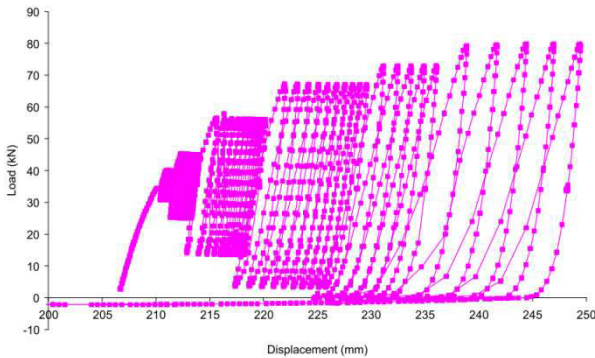


Figure 7. Cyclic loading followed by pull-out (Kelly 2003).

As shown in *Figure 7*, during pull-out tests, maximum tensile load reached was 2.1kN. After the test all the soil remained plugged into the caisson. Maximum tensile load was reached at a vertical displacement of 10-20% of the caisson's diameter. These deformations are too high to satisfy serviceability requirements, so it is suggested that tension limit can be limited to the weight of the caisson plus the weight of the soil plugged inside the caisson and the external skirt friction.

Increasing ambient pressure did not have any effect in these tests, because minimum pore pressure reached under the lid was far from the cavitation limit. The pore pressure may be dependent on the rate of loading and may approach the cavitation limit as rate of loading is increased.

3.3 Transient Vertical Loading of Model Suction Caisson in a Pressure Chamber (Kelly et al. 2006b).

Equipment features

Testing rig and caisson model were the same as utilized by Kelly et al. (2003) at Oxford University. Tests were conducted in pressure chamber using two different sands. Redhill 110 silica sand is the more permeable and it was used to investigate behavior in drained to partially drained conditions. Oakamoor HPF5 is an artificially created sandy silt, and it was used to analyze behavior in partially drained to undrained conditions. Different sands were prepared following different methods of which step by step description is reported in Kelly et al. (2003a and 2003b). Redhill 110 was vibrated till a relative density $D_r=80\%$ with $\phi=43.9^\circ$, density of Oakamoor HPF5 was varying from 53% to 73% with $\phi=48.4^\circ$.

Testing

Caisson was installed by pushing it into the sand at different speeds depending on the sand. In Redhill 110 the caisson was installed at a rate of 0.1mm/s, in Oakamoor HPF5 installation

started with a rate of 0.05mm/s and ended with a velocity of 0.02mm/s. In all tests Installation ended when a preload of 35kN was reached, except for tests number 13 that was preloaded with 15kN.

Each cyclic test consisted of different packets of sinusoidal cyclic loads applied on the vertical axis of the caisson. At the end of the test, the caisson was completely pulled out from the sand. Most of the cyclic tests were made applying a different constant load frequency and varying amplitude, or varying both amplitude and frequency. Two cyclic load tests were carried out with large number of cycles at constant frequency and amplitude, but installing the caisson at different preloading loads. Push-pull tests were carried out pushing the caisson into the sand by steps of 10kN, so dissipation of pore pressure inside the caisson could be investigated, then pull-out displacement was applied at different speeds, varying in a range of 5 - 100mm/s, depending on the test.

Tests carried out in Redhill 110 are summarized on the table below (Kelly et al. 2006b).

Test	Date	Ave. Sample Height (m)	Dry Unit Weight (kN/m ³)	Relative Density	Pressure (kPa)	Cyclic Frequency Hz	Pullout Rate (mm/s)
1	03/04/2003	0.57	15.7	0.79	0	0.5	5
2	11/04/2003	0.56	15.8	0.81	0	1	5
3	28/04/2003	0.56	15.9	0.82	0	-	100
4	30/04/2003	0.55	16.2	0.88	0	-	100
5		0.55	16.3	0.89	0	10	100
6	25/07/2003	0.56	15.8	0.80	200	1	100
7	30/07/2003	0.56	15.8	0.80	0	Multi	100
8	01/08/2003	0.56	15.8	0.80	200	Multi	100
9	04/08/2003	0.56	15.9	0.81	0	-	100
10	05/08/2003	0.56	15.9	0.82	200	-	100
11	06/08/2003	0.56	15.9	0.81	0	-	5
12	07/08/2003	0.56	15.9	0.82	200	0.5	100
13	08/08/2003	0.56	15.8	0.80	200	0.5	100

Tests done in sand Oakamoor HPF5 are summarized in the table below (Kelly et al. 2006b).

Test	Date	Dry Unit Weight (kN/m ³)	Relative Density	Pressure (kPa)	Cyclic Frequency Hz	Pullout Rate (mm/s)
14	25/11/2003	15.1	0.53	0	1.0	5
15	26/11/2003	15.2	0.55	0	0.1	10
16	28/11/2003	15.8	0.67	0	-	100
19	16/03/2004	15.8	0.68	200	0.1	25
20	24/03/2004	15.8	0.67	0	1.0	25
21	26/03/2004	16.1	0.73	0	10.0	25
22	29/03/2004	16.1	0.72	200	1.0	25
23	31/03/2004	16.1	0.72	200	-	25
24	01/04/2004	16.0	0.72	0	10.0	25
25	13/04/2004	16.0	0.72	0	0.1	25

Analyzing cyclic tests in sand Redhill 110, total displacement at the end of each cyclic test is downwards, displacement per cycle increases with load amplitude, and it is greater in the first cycle of every set. The tensile capacity reached was small, in fact, on a target tension load of -5kN only -1kN was mobilized (*Figure 8*). If cavitation limit was not reached, tensile capacity was not affected by the ambient pressure. Varying the loading rate did not affect significantly the load-displacement response. For all cyclic load amplitude, the pore

pressure increased increasing rate of loading and load amplitude.

In the two long cyclic tests ‘shakedown’ effect was noticed. This effect is common for cyclic loading on sand and it causes a decrease in displacement for each cycle as the number of cycles in a series increase. Was not present a significant pore pressure accumulation, and comparison with previous cyclic tests showed that large number of cycles do not affect the load-displacement curve.

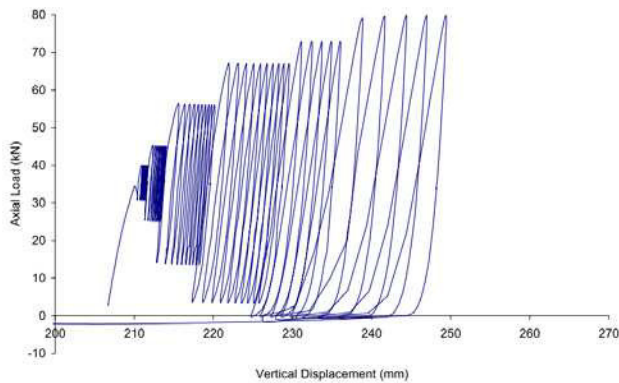


Figure 8. Cyclic loading in Redhill 110 loaded at a rate of 1Hz (Kelly et al. 2006b).

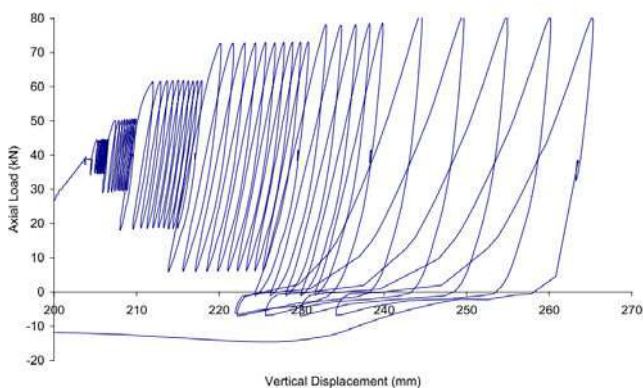


Figure 9. Cyclic loading in Oakamoor HPF5 loaded at a rate of 0.1Hz (Kelly et al. 2006b).

Cyclic tests in sand Oakamoor HPF5 were showing a behavior similar to tests in Redhill 110. Therefore axial stiffness reduced in tension, and ambient pressure did not affect tensile capacity, but the latter reaches a value of -7kN so greater than tests with higher permeable sand. This was due to passive suction developed that was higher than in Redhill 110, and was resisting about 50% of the applied load, against 15% of load resisted by passive suction in tests with sand Redhill 110. Shakedown effect was noticed, as displacement decrease with increasing number of cycles. As for tests in Redhill 110, cyclic amplitude increased as the cyclic load was increasing, and there were greater displacement in cycles where total load were approaching to zero (Figure 9).

Increasing the rate of loading was causing a decrease of downwards accumulated deformation, and an increase in pore pressure development under the lid. The top pore pressure was reached in test 21, at a loading rate of 10 Hz and cyclic amplitude of 25mm/s, where the pore pressure exceeded 350kPa going out of scale.

Push-pull tests in sand Redhill 110, showed that the tension capacity was affected by the rate of loading and was increasing with the increase of ambient pressure. Therefore, unlike cyclic tests, monotonic test was dependent on ambient pressure. An ultimate tensile load of 10kN was mobilized at a displacement of 10mm, corresponding to 3.5% of the diameter of the caisson.

In pull-out tests in Oakamoor HPF5 sand where 5mm/s, 10mm/s, 25mm/s pull-out speed were applied, pore pressure and tensile capacity were increasing with the pull-out velocity. Ultimate tensile load of 10 kN was mobilized at a displacement of 7% of the caissons diameter. The maximum load was related to the rate of pull-out and limited by cavitation, so greater pull-out velocity and ambient pressure were allowing larger loads.

3.4 A Comparison of Field and Laboratory Tests of Caisson Foundation in Sand and Clay (Kelly et al. 2006a).

Equipment features

Same equipment and preparation procedure of Byrne (2000) were used in this work. Tests were carried out with sand Redhill 110 and prepared with relative density in the range of 70% to 84%. Two caisson models with aspect ratio of 0.66 and different diameters of 20mm and 15mm were used to carry out tests where vertical cyclic loading was applied.

Testing

Different modality of installation were applied in tests with 15mm diameter caisson. In one test the caisson was installed by suction and in the other by pushing, till a preloading of respectively 0.065kN and 0.062kN was reached. Installation of 20mm model caisson was done by pushing till a preload of 0.152kN. In each test a cycling load package with increasing amplitude was applied.

Since different caissons were utilized, results were converted into dimensionless form in order to allow comparison. Cyclic tests carried out with different caissons dimension and installed pushing, were showing that larger caisson had less accumulated displacement, so increasing the scale brings to a decrease of total displacement.

As can be seen in Figure 10, tests where installation was done by suction, had a significantly higher total downward displacement. Stiffness was decreasing increasing load amplitude, and was remaining constant in sets of cycles with the same amplitude. Hysteresis was increasing with cyclic amplitude, and this increase was more marked when the load become tensile.

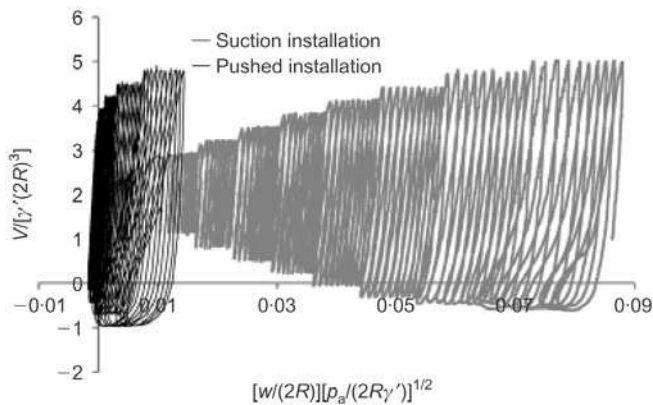


Figure 10. Cyclic loading after suction and pushed installation (Kelly et al. 2006a).

3.5 Centrifugal Experiment Study of Suction Bucket Foundations under Dynamic Loading (Lu X. et al. 2007).

Equipment features.

In this work a 50g-ton centrifuge was used to carry out tests. Sample of fine sand was prepared in a 600mm x 350mm x 350mm (L x W x H) tank. Sand was prepared layer by layer and pore pressure transducers were placed in between each layer, inside and outside the suction caisson, following a defined pattern. Sand was then saturated flushing water inside from the bottom, and applying vacuum. Consolidation was done applying a pressure of 80g, reaching a dry density of 15.69kN/m³. Displacement measurements were done by means of two LVDT connected at the top of the caisson and another placed on the sand surface. Suction caissons had a diameter of 60mm and different skirt length of 48mm, 72mm, and 90mm. Vertical load was applied by hydraulic-electric system that can develop a maximum force of 0.98kN and a maximum frequency of 20Hz.

Testing

Monotonic tests were carried out with 60x48mm caisson, applying an upward displacement of 10 mm in steps of 0.2 mm. The uplift bearing capacity was mobilized at a displacement of 3.5 mm, corresponding to 2.1% of the diameter of the caisson, reaching a tension load of 0.59 kN. Uplift velocity is not specified in the article.

Cyclic tests were done by applying displacement amplitude of 2mm, 1mm, 0.5mm, and 0.2mm, at a frequency of 0.8Hz. Greater amplitude allowed greater pore pressure, of which peak was reached after 2.5 hours of loading, then the pore pressure was remaining constant with a slight decrease over the time. As a general behavior, great pore pressure was developed below the lid, pore pressure was decreasing with the depth and with distance from the model caisson. Applying an amplitude of 2mm (67% of the static uplift capacity) was bringing to a total liquefaction of the soil, with a reduction of the liquefied layer thickness decreasing the load.

3.6 Experimental Study on the Bearing Capacity of Suction Caissons in Saturated Sand (Lu et al. 2009).

Equipment features.

Tests were carried out in a 500mm x 500mm x 500mm tank made of glass, filled with 400mm of water saturated Mongolia sand that was vibrated in order to reach a dry density of 15.69kN/m³. Displacements were measured by a LVDT with a range of 0-30mm and loads were measured by a transducer with a range of 0-6kN. Because of the limit of the apparatus, the vertical load was applied by displacement at a rate of 0.0067mm/s.

Two typology of foundation were tested, a monopod with diameter of 40mm and skirt length of 72mm and a tetrapod, composed of four caissons of the same dimension of the monopod, positioned at a distance of 10mm to each other. Each model caisson had a valve on the top that could be closed or opened depending on which test was carried out.

Testing

Monotonic compressive tests were carried out with a target downward displacement of 20mm. The bearing capacity curve had a steep increase during the first 4mm, then the increase become more slight. Single caisson reached a bearing capacity of 240N when the valve at the top was sealed, and a bearing capacity of 210N when the top valve was open. The difference is low because under monotonic loading the behavior of the sand tended to be drained also when the valve was sealed. Response of the tetrapod was nearly 4 times the response of monopod, meaning that bearing capacity was increasing with the same proportion of the numbers of suction caisson installed.

Monotonic tensile tests were carried out with both monopod and tetrapod, applying uplift vertical displacement at different rates (0.016mm/s, 0.16mm/s, 0.32mm/s). Uplift bearing capacity increased with the rate of loading (Figure 11). The bearing capacity of tetrapod was almost 6 times the bearing capacity of the monopod, so there was a high strengthening effect using tetrapod configuration.

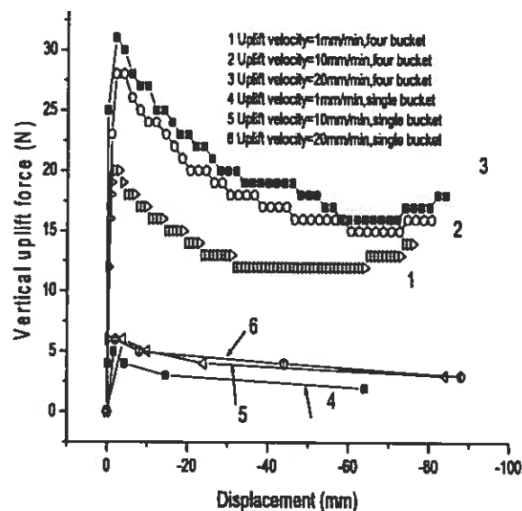


Figure 11. Load-displacement curve of single and four-caisson model under uplift loading (Lu et al. 2009).

3.7 Axial Capacity of Suction Piles in Sand (Jones W.C. et al. 1994).

Equipment features

Hydraulic ram was used for vertical loading. A cylindrical tank, with a diameter of 914mm and 1060mm high, was filled by Oklahoma sand, saturated with de-aired water in test where water saturated sand was used. Displacements were measured by a LVDT and load measurements were done by means of electronic load cell. A double-walled model caisson was used. The caisson was designed so that pore pressures can be measured both inside and outside the caisson, by pressure transducers placed in three different positions on both sides of the skirt. Inner diameter of the caisson model was 111mm and outer diameter was 127mm.

Testing

Installation was carried out both by pushing and by suction. In installation by pushing 667N were required to complete the procedure for all the skirt length, and it was calculated that 91% of the installation load was carried by tip resistance. In installation by suction the first step was to let the model caisson to penetrate under its own weight. After self-weight penetration, different active suction were applied in different tests, in order to determine the minimum value of negative pressure required for installation, found to be 3.1kPa. Despite suction was maintained at the minimum value allowing installation, liquefaction of the soil inside the caisson could not be avoided, and an excess soil plug of 50mm was formed not allowing a complete penetration. Force required installing by suction was of 80N, therefore significantly lower than pushing installation. This was due in part to the not complete installation, but mainly to the flow around the skirt occurring as consequence of pressure gradient.

After suction installation, pull-out tests were carried out at a constant pull-out rate of 76mm/s. Tests in drained conditions were carried out in dry sand, keeping valve at the top of the model caisson open. The maximum tensile load was 66N, 50% of which was due to the caisson weight, and was mobilized at a displacement of 0.8mm (0.7% of the caisson diameter). Test in partially drained conditions were carried out in water saturated sand. Maximum tensile load of 244N was reached at a displacement of 25.4mm.

Tension load was causing a decrease on stiffness. Positive and negative pore pressures were increasing in magnitude as the load was going respectively in compression and tension. This increase was not due to the increasing load, but was depending on the velocity that the actuator had to apply in order to reach the target load within a period of 1 second.

3.8 Suction Caissons in Sand as Tripod Foundations for Offshore Wind Turbines (Senders 2008).

Equipment features.

Tests were carried out in a 40g-tones centrifuge, equipped with a sand box of 650mm x 390mm x 325mm (L x W x H). Electrical actuator was used to apply vertical displacement, maximum load capability was of 8kN and it could move in a

range of 240mm. Further details are described in *Randolph (1991)*. Loads were measured by a 10kN load cell and pressure was measured by pore pressure transducers connected inside and outside the caisson. A syringe pump was used for suction installation.

Model caissons used in sand had skirt length/diameter measures of 60/60mm, and 60/49mm. Both of them were equipped with two valves: one to let the water going out and the other to apply suction by means of the syringe pump. Tests were carried out in oil saturated silica sand, the sample was then vibrated so a relative density in a range of 90-100% was reached.

Testing

Installation was done both by suction and by pushing at the rate of 1mm/s. Pull-out tests were carried out in both drained and undrained conditions, keeping the valve respectively open and closed, and applying slow or fast rate of loading. Cyclic tests were carried out to analyze partially drained to undrained conditions so valves were kept closed.

Monotonic pull out

Pull-out tests were carried out at 100g, keeping the valve open and applying slow pull-out rate for drained tests, and keeping the valve close and high pull-out rate for undrained tests.

In both drained and undrained tests, pore pressure response was increasing with up-lift velocity, and cavitation was reached with an uplift speed of 5mm/s. Seeing results in *Figure 12*, it was concluded that the uplift resistance increased increasing the pull-out rate, for infinitely slow (valve open), 1mm/s, and 5mm/s uplift speeds, the pull-out resistance was respectively $1.13\gamma 'D$, $1.63\gamma 'D$, $2.45\gamma 'D$, values consistent with findings from *Bye et al. (1995)* and *Houlsby et al. (2005b)*.

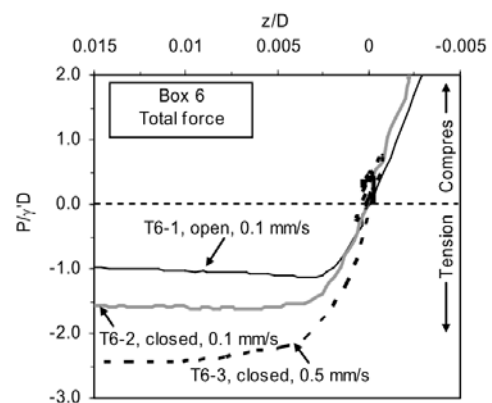


Figure 12. Total resistance (Senders 2008).

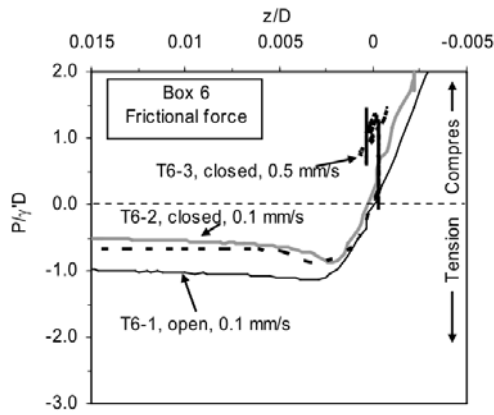


Figure 13. frictional resistance (Senders 2008).

Figure 13 shows resistance given by friction in undrained tests, calculated subtracting uplift resistance given by pore pressure at the total response. Frictional resistance reached peak almost immediately (Figure 13), with a linear trend, and was greater in drained condition. In undrained condition frictional resistance was decreasing after the peak, till a value that was half of the drained ones. The initial linear behavior of frictional resistance was similar for all tests, so it seemed to be not affected by up-lift velocity.

Figure 14 is showing the force developed by passive suction below the lid. There was a slight difference between tests carried out at different speed, therefore it was concluded that pore pressure was not directly related to the uplift speed. Comparing pore pressure with friction resistance, it was noticed that the latter was mobilized immediately, instead for the former the process was slower.

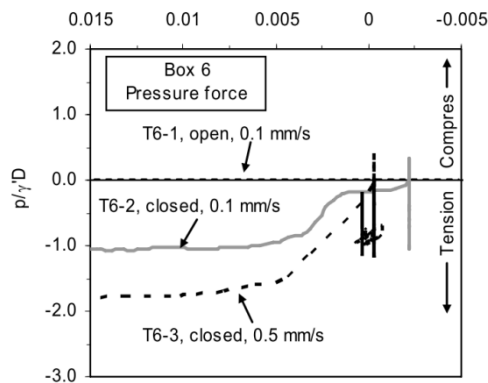


Figure 14. Pore pressure force below the lid (Senders 2008).

Cyclic loading

Cyclic loading tests were carried out keeping the valve on the lid closed and at an acceleration of 100g. Load cycles amplitude and frequency were varying between and within tests. Low frequency tests were carried out in a range of 0.07-0.045Hz, while in high frequency tests, loading frequency was in a range of 1-10Hz. Each cyclic test ended with tensile failure, and frequency, mean load, and load amplitude were

varied individually if initial settings of cyclic loading were not critical enough to cause failure (Figure 15).

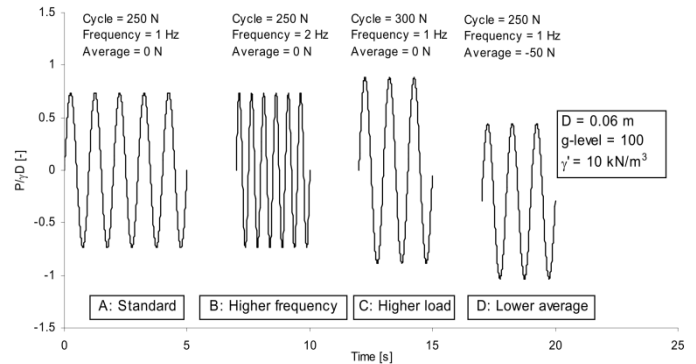


Figure 15. Example of several cyclic loading patterns (Senders 2008).

Tests where large number of cycles was applied were showing that the number of cycles was not affecting the degradation of resistance, and it was not causing softening of the response. Also when cyclic load of 5N less than the static uplift resistance was applied, number of cycles did not affect degradation of resistance, and a steady state was reached between cyclic differential pressure and number of cycles. Conversely to the current design practice of suction caissons, it was concluded that resistance degradation due to large number of cyclic load does not need to be taken into account for the design.

3. DISCUSSION.

Kelly (2006b) used two different sands to evaluate the behavior under tensile loading. In both cases, greater load is mobilized at smaller displacement in only pull-out tests with respect to cycling followed by pull-out tests, showing that loading history heavily affects the response. On cycling followed by pull-out tests, greater displacement is required to mobilize smaller load because of the loosening of sand below the lid. Byrne (2000) showed that loading history can also bring to an increase of the relative density, affecting positively the pull-out response.

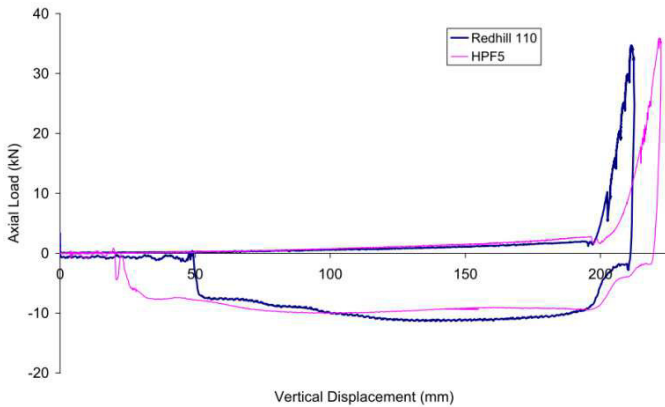


Figure 16. Pull-out response of large displacement test (Kelly et al. 2004).

From monotonic pull-out tests, carried out by Byrne (2000), where rate and displacement magnitudes are varied, it is concluded that there are different phases of the response as can be seen in Figure 5. Same different phases of the response can be noticed also in Figure 16, where Kelly (2006b) analyzed the behavior under rapid pull-out in drained and partially drained soil conditions, respectively with sands Redhill 110 and HPF5. The initial softening behavior of the soil, occurs in this latter work at a greater tension load with respect to Byrne (2000). Comparing tests carried out at atmospheric pressure, in Kelly (2006b) and Byrne (2000), the differences are in pull-out speed, caisson diameter, and fluid of saturation. Larger caisson and greater pull-out speed utilized in Kelly (2006b) bring to a greater pore pressure development which could be the reason why the softening behavior occurs at greater tension load in this latter work. Since less frictional resistance is expected in the oil saturated sand, softening behavior is expected to occur at less tension load. Greater frictional resistance occurring in Kelly (2006b) can confirm the conclusion of Byrne (2000), who stated that the softening behavior occurs when the load exceed the skirt friction resistance. Byrne (2000) suggested that this softening behavior needs to be studied or in a geotechnical centrifuge, or with larger caisson in a sample hydraulically surcharged, in order to increase total stresses. Tests carried out in centrifuge and in a sand sample hydraulically surcharged using larger caisson were carried out respectively by Senders (2008) and by Manzotti et al. (2014). Softening behavior has been noticed only in the latter work, and is more marked in test where overburden pressure is applied. Softening behavior

is not present in Senders (2008), despite the fact that drained tensile capacity is greater than Byrne (2000). This suggests that further studies are needed in this topic.

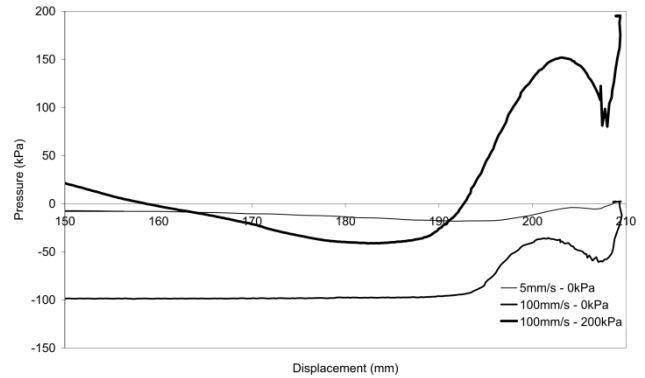


Figure 17. Pressures beneath the lid of the caisson during ultimate tensile loading in Redhill 110 sand (Kelly et al. 2006b).

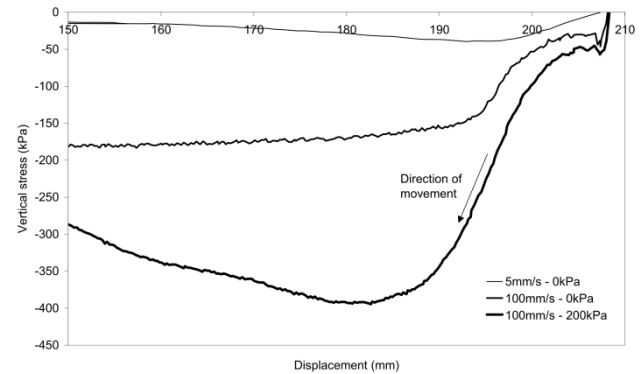


Figure 18. Ultimate tensile loading in Redhill 110 sand (Kelly et al. 2006b).

In Kelly (2003) and Kelly (2006b) tensional capacity under rapid loading in a pressure chamber was analyzed. At low pull-out rates, the response is drained and the capacity is given by the friction on the skirt. Increasing the rate of loading brings to a partially drained behavior, causing an increase of both stiffness and pore pressure (Figure 17 and Figure 18). The response becomes greater and is limited by cavitation. Therefore, when the ambient pressure increases, the capacity is limited at higher loads, since it is increased the pressure at which cavitation occurs. The ambient pressure affects only the limit of the capacity, not the capacity inside the limit. Ultimate tensile load is dependent on the suction that can be generated under the lid. Hence, in order to have a high tensile load in sand with low permeability, a fast rate of loading and high ambient pressure are needed.

As pointed out by Senders (2008) and Byrne (2000), the uplift resistance in drained condition is given by friction on the inside and outside of the skirt. Friction resistance is mobilized with small displacement of the caisson with respect to the passive suction resistance (Byrne 2000, Kelly 2006b). As the behavior become more undrained, less

frictional resistance is mobilized and more load is carried by passive suction. In these conditions the ultimate tensile capacity is mobilized with smaller displacement, but always at a greater displacement with respect to the frictional resistance. *Houlsby et al. (2005b)*, shows that high passive suction is mobilized at displacements in a range of 10 to 23% of the caisson diameter, therefore out of serviceability requirements.

Jones (1994) showed that in partially drained condition, suction developed below the lid cause a downward flow outside the skirt, which increases the effective stresses and so the frictional resistance on the outside skirt. In *Kelly (2006b)*, in tests carried out in Oakamoor HPF5 sand, greater load is mobilized with a pull-out rate of 10mm/s than 100mm/s. Since passive suction developed beneath the lid is smaller in the first test, this suggests that less skirt friction is mobilized in the test with a pull-out rate of 100mm/s. Comparing this latter test with test carried out in Redhill 110 sand, maintaining the same pull-out rate and the same caisson, maximum tensile load is mobilized at greater displacement in the less permeable sand Oakamoor HPF5 (*Figure 16*), where a partially drained to undrained behavior occurs. This behavior is in accordance with the conclusion that the enhancement in skirt friction due to the external downward gradient does not have time to occur in totally undrained condition.

It can be concluded that the ultimate tensile load increases proportionally to the uplift speed and the permeability of the soil, as long as the partially drained behavior allows the hydraulic gradient to occur. This is in accordance with Darcy law which linearly related the seepage with pressure differential. Tests carried out in pressure chamber (*Kelly 2003, Senders 2008*) shows that ultimate tensile load is mobilized at a displacements around 10-20% of the caisson diameter, therefore too large to satisfy serviceability requirements.

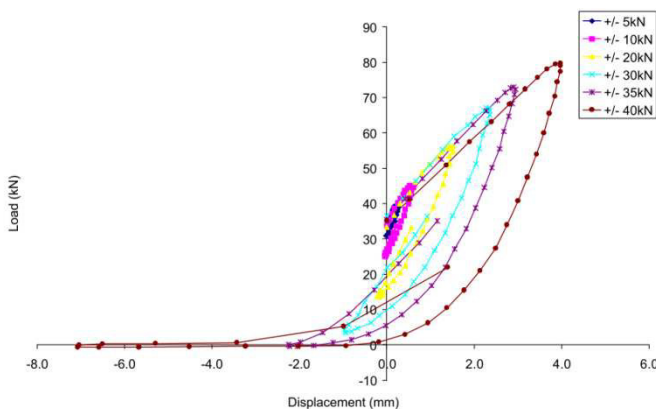


Figure 19. Cyclic loading carried out at different amplitudes (*Kelly 2003*).

In agreement with *Byrne (2000)*, during cyclic loading in *Kelly (2003)* the vertical stiffness of the caisson is significantly lower in tension than in compression, as can be seen from *Figure 19*, that gives a great representation of a typical load-displacement behavior under cyclic loading. This

behavior is noticed also in *Kelly (2006b)*, where a typical trend of results, shows that for small cyclic load amplitude the response is stiff. As the amplitude increases and the load goes into tension, it turns in less stiff response. This brings to an increase of accumulated downward displacement and hysteresis. The physical meaning of increase in hysteresis is the increase in damping. This behavior has to be avoided in stage of design, so traction has to be avoided (*Houlsby 2005b*). *Kelly (2003)* found that the boundary of this dropping, rather than the transition into tension, is when the drained frictional capacity of the skirts is exceeded. Cyclic tests in *Byrne (2000)* and *Kelly (2006b)* are confirming these findings, showing tests where, despite the tension load is not reached, there is a significant drop in stiffness close to 0kN. In the less permeable sand, where less friction is mobilized, this drop occurs around 3kN as shown in *Figure 20*.

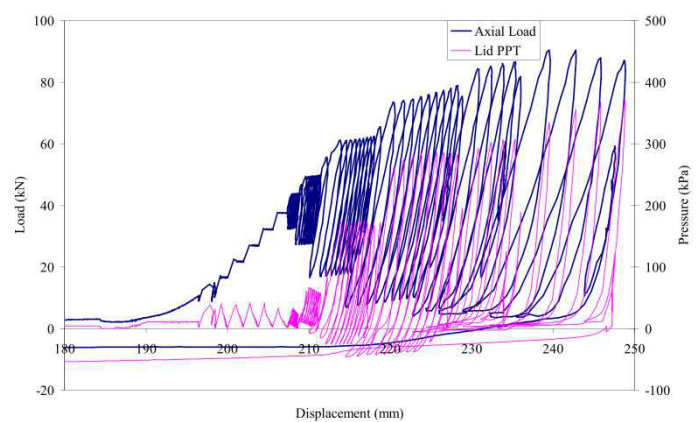


Figure 20. Load-displacement curve of test 14 (*Kelly 2006b*).

As general behavior in cyclic tests, ultimate tensile load is mobilized at displacement that compromise the serviceability of the structure, and in *Kelly (2006b)* it is stated that the low stiffness reached when tension load is applied can impose serviceability design limit.

This fast decrease in stiffness could be a reason to limit the design tensile load on an up-wind leg of a multi-pod foundation to the self-weight of the caisson plus the internal and external skirt friction, otherwise, due to the low stiffness, there could be ratcheting into the soil (*Kelly 2003*). Avoid tension in a multi-pod foundation can be done adding ballasting or increasing the spacing between legs. Since these solutions are affecting the cost of the structure, to reduce conservatism *Senders (2008)* and *Kelly (2003)* suggest that tension could be allowed under extreme condition.

According with *Bye (2005)*, in *Senders (2008)*, a faster and higher development of pore pressure was noticed in high frequency cyclic tests with respect to low frequency tests. This is in contrast with founding in *Byrne (2000)*, *Mangal (2000)* and *Johnson (1999)*, who stated that the influence of loading rate is negligible. Rate dependency is evident also in *Kelly (2003)*, where decreasing the rate of loading in partially drained conditions brings to a decrease in pore pressure development. Pore pressures are increasing with the rate of

loading also in drained tests, but are not affecting the load-displacement behavior (Test 7 in Kelly et al. 2006b). This response could be explained by the less relevance that passive suction has in a drained response. Kelly (2003) found that pore pressure is linearly related to velocity when the load remains in compression. As a tension load is applied, the increase of differential pressure with the increase of loading frequency is not linear anymore and is found to be inversely dependent on the soil permeability.

In cyclic tests, total displacement is downward and increases when the load goes into traction. This behavior has been confirmed in various articles (Kelly 2006b, Byrne and Houlsby 2002a and Byrne 2000), and is attributed by Byrne (2000) to the loosening that occurs during tensile load, that brings to greater displacement when load becomes compressive. It has to be noticed that in these studies the mean load is compressive also when traction is applied. In Kelly (2006b) tests carried out in a pressure chamber are showing that ambient pressure does not affect load-deformation response in cyclic tests, but affects only the limit of pull-out tension capacity.

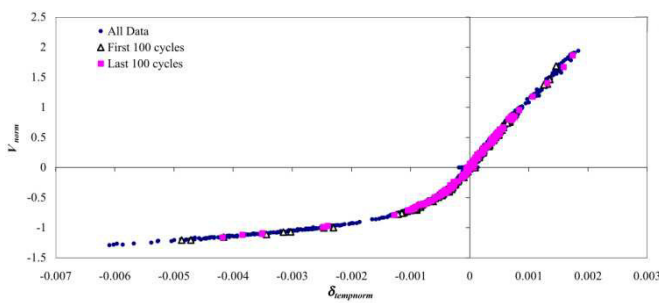


Figure 21. Long cycle response (Byrne 2000).

Lu (2007) established that cyclic response goes gradually in a steady state, where pore pressure fluctuates around a constant value and displacement does not develop any further. Similar behavior is noticed also in Byrne (2000) where, in order to evaluate how many cycles are necessary to carry out cyclic tests, a test with 2000 cycles was carried out. In this latter test, no significant difference in response is noticed between the first and the last 100 cycles as can be seen in Figure 21, showing that 100 cycles are enough to reach the steady state mentioned by Lu (2007). It is also noticed that when a cyclic load is applied, in between cycles with the same amplitude the stiffness remains constant (Byrne 2000). A more close analysis on stiffness in long cyclic tests is done by Kelly (2006a), where stiffness is noticed to increase, slightly and with a decreasing rate, with the number of cycles till a steady state is reached. These considerations are true as far as the load does not approach 0kN, at which point the stiffness drops. It is important to conclude that during cyclic loading there is no degradation of the response, but a little recovery on stiffness occurs instead.

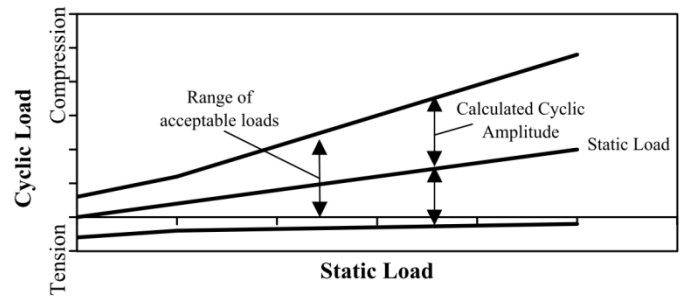


Figure 22 cyclic bearing capacity (Bye et al. 1995).

Figure 22 shows a graph extrapolated from field tests by Bye et al (1995), where value on axis was not shown since results of the study are confidential. This graph suggests that there are boundaries limiting cyclic load amplitudes that can be sustained, once these boundaries are exceeded a rapid degradation occurs, so extreme events have been inserted to study this behavior in Byrne (2000). This clear threshold was not present in tests summarized in the present work, where in cyclic loading tests there is a gradual transition from stiff symmetric response to an asymmetric response as the load approaches tension, and, even after a tension load, the degradation is still gradual. The tensile boundary suggested by Bye et al. (1999) in Figure 22 may be placed between the initial soft response and the rate-dependent response of the pull-out loading shown in Figure 5 (Byrne 2000).

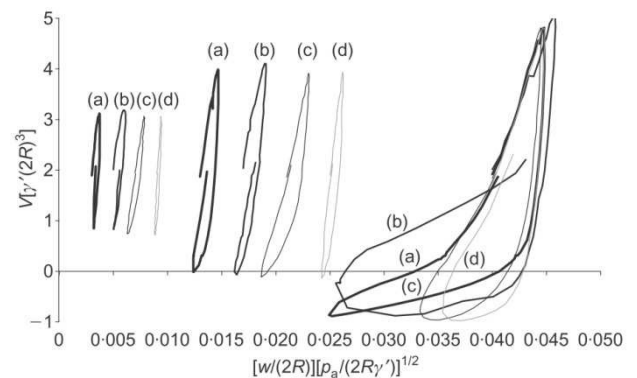


Figure 23. Comparison suction and push installation: installations by suction a) field test, b) 150 mm diameter caisson installed by suction, c) 200 mm diameter caisson installed by pushing, d) 150 mm diameter caisson installed by pushing. Kelly (2006a).

Responses of loading on caisson installed by suction and by pushing are showed in Figure 23, where results are normalized in order to allow a comparison. Tests where installation is done by suction have higher total downward displacement and a more steep decrease on stiffness. This behavior is due to loosening of sand that occurs along the skirt during installation, causing a reduction on the frictional capacity. Since these disturbances are localized, they have more relevance in small scale tests, causing greater displacement, in proportion with larger scale models. This

latter consideration is true also for caisson of different dimension installed by pushing, as noticed in *Byrne (2000)* where normalized displacements are larger for smaller diameter caisson. *Jones (1994)* found that, applying suction installation, the penetration resistance is reduced to about one third with respect installation by pushing. In this latter work it is concluded that frictional capacity during pull-out loading of the caisson is reduced by suction installation, but has to be noticed that complete penetration into the soil cannot be done, because of formation of a soil plug inside the caisson. These considerations about how the modality of installation in laboratory affects the pull-out response, need to be further investigated, since phenomena that can act in favour of tension resistance, as consolidation of the soil occurring time after installation, has not been considered. In order to have, in pushing-installation test, a tensile behavior more similar to suction installation, it is suggested to study a loading history that cause a disturbance of the soil along the skirt similar to the one caused by suction installation, relying on passive suction to activate the flow mechanism near the skirt. Keeping in mind that to reach a steady state long cyclic test is not necessary, a cyclic test that ends with a steady state that induce a degradation comparable with the one of suction installation is possible.

4. REFERENCES.

- Bye, A., Erbrich, C. and Rognlien, B. (1995), Geotechnical Design of Bucket Foundations, OTC paper 7793, pp 869-883.
- Byrne, B.W. and Houlsby, G.T. (2002), Experimental Investigations of the Response of Suction Caissons to Transient Vertical Loading, Proc. ASCE Journal of Geotechnical engineering 128 N°11, pp 926-939.
- Byrne, B.W., Houlsby, G.T., Martin, C.M. and Fish, P.M. (2002a) "Suction caisson foundations for offshore wind turbines." Wind Engineering, Vol. 26, No 3.
- Byrne, B. W. & Houlsby, G. T. (2003) Foundations for offshore wind turbines. Philosophical Transactions of the Royal Society of London Series A, Vol. 361 , pp 2909-2930.
- Byrne, B. W. (2000) Investigations of suction caissons in dense sand. PhD Thesis, Magdalen College. London, Oxford, United Kingdom.
- Houlsby, G. T. & Byrne, B. W. (2005) Calculation procedures for installation of suction caissons in sand. Geotechnical Engineering 158 , pp 135-144.
- Houlsby, G. T. and Cassidy, M. J. (2002) A plasticity model for the behavior of footings on sand under combined loading. Geotechnique, 52 , pp 117-129.
- Houlsby, G. T., Ibsen, L. B. and Byrne, B. W. (2005a) Suction caissons for wind turbines. Proc. International Symposium 'Frontiers in Offshore Geotechnics'. Perth, Australia, Taylor & Francis Group.
- Houlsby, G. T., Kelly, R. B. and Byrne, B. W. (2005b) The tensile capacity of suction caissons in sand under rapid loading. Proc. International Symposium on Frontiers in Offshore Geotechnics (ISFOG). Perth, Australia, Taylor & Francis Group.
- Houlsby, G. T., Kelly, R. B., Huxtable, J. & Byrne, B. W. (2006) Field trials of suction caissons in sand for offshore wind turbine foundations. Geotechnique, 56 , pp 3-10.
- Jiao B., Lu X., Zhao J., Wang A., Shi Z., and Zeng X H, (2009), Experimental Study on the Bearing Capacity of Suction Caissons in Saturated Sand. Institute of Mechanics, Chinese Academy of Sciences, Beijing 100080, China.
- Johnson, K. (1999), The Behavior of Partially Drained Footings under Axial Load, 4th year project report, University of Oxford, United Kingdom.
- Jones W.C., Iskander M.G., Olson R.E., and Goldberg A.D. (1994) Axial Capacity of Suction Piles in Sand, Offshore Technology Research Center, pp 63-75.
- Kelly, R. B., Byrne, B. W., Houlsby, G. T. & Martin, C. M. (2003). Pressure chamber testing of model caisson foundations in sand. Proceedings of the international conference on foundations, Dundee, pp. 421-431.
- Kelly, R. B., Byrne, B. W., Houlsby, G. T. & Martin, C. M. (2004). Tensile Loading of Model Caisson Foundations for Structures on Sand, . Department of Engineering Science, University of Oxford, United Kingdom.
- Kelly, R. B., Houlsby, G. T. & Byrne, B. W. (2006a). A comparison of field and laboratory tests of caisson

- foundations in sand and clay. *Getotechnique*, 56, No. 9, 617–626.
- Kelly, R. B., Houlsby, G. T. and Byrne, B. W. (2006b). Transient vertical loading of model suction caissons in a pressure chamber, Report OUEL 2291/06. Department of Engineering Science, University of Oxford, United Kingdom.
- Lesny, 2010. K. Lesny. Foundations for Offshore Wind Turbines. ISBN 978-3-86797-042-6, Tools for Planning and Design. VGE Verlag GmbH, 2010.
- Lu X., Wu Y., Jiao B., Wang S. (2007), Centrifugal Experiment Study of Suction Bucket Foundations Under Dynamic Loading. Institute of Mechanics, Chinese Academy of Sciences, Beijing 100080, China.
- Mangal, J. (1999), Partially Drained Loading of Shallow Foundations on Sand, DPhil Thesis, University of Oxford, United Kingdom.
- Murff, J.D. (1996). “The geotechnical centrifuge in offshore engineering,” OTC 8265. Proceedings, 28th Annual Offshore Technology Conference. 1, 675-689.
- Randolph, M. F., Jewell, R. J., Stone, K. J. L. and Brown, T. A. (1991) Establishing a new centrifuge facility. Inko, H. Y. and Mclean, F. G. (Eds.) Centrifuge 1991. Boulder, Colorado, A.A. Balkema.
- Randolph and Gouvernec, 2011. M. Randolph and S. Gouvernec. Offshore Geotechnical Engineering. ISBN 978-0-415-47744-4. Spoon Press, 2011.
- Roy E. Hunt, (2010) Characteristics of Geologic Materials and Formations: A Field Guide for Geotechnical Engineers. CRC Press.
- Senders, M., (2005) Tripods with Suction Caissons as Foundations for Offshore Wind Turbines on Sand, University of Western Australia.
- Senders, M., (2008) Suction Caissons in Sand As Tripod Foundations for Offshore Wind Turbines, Ph.D. Thesis, University of Western Australia.
- Sørensen P.H.S., Brødbeck K.T., Møller M. and Augustsen A.H. (2012), Review of Laterally Loaded Monopoles Employed as the Foundation for Offshore Wind Turbines. Department of Civil Engineering, Aalborg, Denmark.
- Tran M.N., Randolph M.F., and Airey D.W., (2005), Study of Sand Heave Formation in Suction Caissons Using Particle Image Velocimetry (PIV), Centre for Offshore Foundation Systems, University of Sydney, Sydney, Australia, University of Western Australia, Perth, Australia.

Laboratory Setup for Vertically loaded Suction Caisson Foundation in Sand and Validation of Responses

Aalborg University, Department of Civil Engineering, Denmark

Abstract: Wind energy obtained by means of wind turbine has been proved to be a concrete resource of green energy. Development of such structures requires research on offshore construction, since this is the direction for future improvement on this field. Wind turbines are relatively light and slender devices usually installed in farms, therefore many inexpensive foundations are needed. Suction Bucket foundations are a suitable option for this purpose, but for large scale utilization more research is required, especially for in-service performance. Size of offshore wind turbine has been increasing during the last years and, following this trend, design choice will turn into foundation composed of three or four suction bucket foundations, called respectively tripod and tetrapod. Overturning moment in tripod and tetrapod is carried by vertical loading, therefore vertical pull-out capacity is tested, in both static and cyclic case of loading. Testing rig and equipment are presented together with procedures. Some tests results are presented in order to verify the output of tests. CPT-based methods and beta-methods to evaluate vertical installation and pull-out response are then presented and implemented in Matlab in order to validate responses.

1. INTRODUCTION.

Nowadays wind turbines have been proven to be a reliable source of 'green energy'. Onshore installations are present but not always possible, because of the impact on the landscape and large areas required. Wind turbines are therefore preferably installed offshore, where larger structures can be realized, and more stable wind allows a more regular production (Byrne et al, 2003). A drawback of offshore installations is the greater load given by wind and waves, and the installation procedure, although the latter can cause problems also in onshore installation.

Such light structures like wind turbines, are subjected to small vertical load, compared to the overturning moment caused by waves and wind. Wind turbines are usually founded on piles. This typology of foundation is well known and of simple design, but is considered expensive, since represents the 35% of the total cost of the installed structure (Byrne et al, 2003). Cost is always an important issue, especially for offshore wind turbine that has been shown to be a reliable source of renewable energy with a great potential of expansion in the market. Suction caisson foundation, also called suction bucket foundation, is an alternative solution for offshore foundations. Alternative that allows to decrease the total cost of the structure, requiring less material and less cost in terms of construction and installation, compared to pile foundation.

A suction caisson foundation has the shape of an upturned bucket, with an aspect ratio, length over diameter (L/D), less than one for structures installed in sand. The installation consists of two main steps: first, the foundation penetrate the soil under its own weight, then suction is applied, reducing

the pressure inside the bucket, and allowing the complete insertion of the caisson into the soil.

In light and slender structures such as wind turbine, horizontal load in extreme condition may reach 60% of the vertical load (Houlsby et al, 2005c), making overturning moment on the foundation the main concern. Bucket foundations are installed both as monopod (single structure) or tripod/tetrapod (multiple foundation). In the first case overturning moments are resisted directly by the rotational capacity of the foundation, in the second case overturning moments are transmitted to the foundation by transient tension and compression vertical loads, on the respectively upwind and downwind legs. The accumulated deformation under cyclic loading is the main issue of interest during design of both monopod and tripod/tetrapod, since can brings to serviceability problems (Byrne et al, 2003; Kelly et al, 2005).

In general, physical models are an approximation of real natural condition, given that a laboratory set up is always subjected to laboratory effects and scale effects. Laboratory effects are due to the difficulty of reproducing the physical condition found in nature, as environment surroundings and loads. To overcome this problem, the sand box used in tests presented in this article has dimensions designed in a way that does not interfere with the bucket installed in its centre, and therefore gives a faithful reproduction of seabed. Scale effects increase increasing the scale factor, since quantity that cannot be scaled such as gravity, viscosity, grain size, etc. affect results of scaled quantities. The equipment of Aalborg University laboratory has a scale factor approximately of 1:10, allowing low scale effects.

Testing setup presented in this article, is made to investigate the behaviour of foundations subjected to vertical loads in sand. In this work, only procedures to test bucket foundations

are discussed, despite that, the system is suitable also for other typologies of foundations, such as monopiles. By MOOG program a wide range of static and cyclic loads can be applied, and the sand box equipment allow to apply overburden pressure by suction. In the case of study only tensile vertical loads will be applied, with and without overburden pressure. Therefore typical loads to which are subjected the upwind legs of a multiple foundation is simulated.

In literature, various design methods has been proposed in order to evaluate installation and pull-out resistance of suction caisson in sand. In this study, responses from installation and pull-out tests carried out at Aalborg University are utilized to compare results from different methods. Effect of suction is not considered because this phenomenon is not present during installation and has a marginal importance on pull-out response in drained condition. Beta-methods and CPT-based methods of interest are presented. Then methods are analyzed and validate, grounding on experimental responses.

2. EQUIPMENT.

Tests are carried out in the geotechnical laboratory of Aalborg University, structure of the equipment used is shown schematically in *Figure 1*.

The testing rig includes a rigid circular box, a movable loading frame equipped with two movable hydraulic pistons, a signal transducers box and a measuring system described in the following.

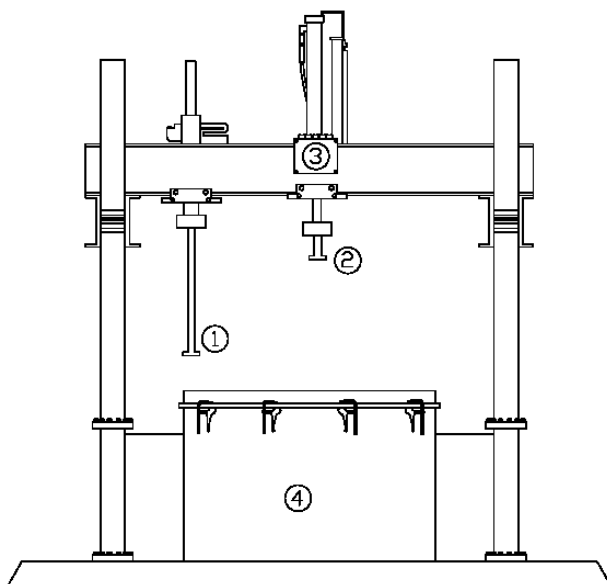


Figure 1. Equipment used testing bucket foundation: loading piston (1), installation piston (2), signal transducers box (3) and sand box (4).

Testing system shown in *Figure 1* is described together with equipment for specific testing of bucket foundation.

2.1 Sand box

The sand box is a steel made cylinder with a diameter of 250 cm and a total height of 152 cm. A 30 cm thick layer of gravel with high permeability is placed at the bottom, in order to provide a uniform distribution of water and create uniform water pressure, avoiding piping problems. A geotextile sheet is placed on top of the gravel layer, to avoid sand infiltration and thus maintain drainage property unaltered. The top layer is composed of Aalborg University Sand No.1 and has a thickness of 120 cm. Water is leaded into the box by a system of perforated pipes, uniformly placed on the bottom.

To supply water a tank of 1 m³ is filled of water and placed in a higher position with respect to the sand box. This allows having an upward gradient in the sand box, needed to loosen the sand. The in and out flow of water is controlled by a system of valves shown in *Figure 2*. Regulating the inflow valve, the level of gradient in the sand box is regulated and measured with a piezometer, on which a mark is made in order to have a gradient of 0.9.



Figure 2. In and out flow valves.

2.2 Bucket Models.

Two cylindrical shaped models of bucket foundation have been built to be tested. Both models have an outer diameter of 1000 mm, and a wall thickness of 3 mm, the skirt length is 500 mm for M1 (aspect ratio $L/D=0,5$), and 1000 mm for M2 ($L/D=1$). Models are approximately scaled of 1:10.

Each model is composed of two parts. The first component is a steel made bucket, with a thickness of 3 mm, the second component is a steel plate placed above the lid of the bucket, with a thickness of 20 mm (*Figure 3*). The steel plate is connected to the bucket by eight bolts and a rubber gasket is installed along the diameter, this connection is made to make possible to place the elastic membrane in between, when a test with suction is run.

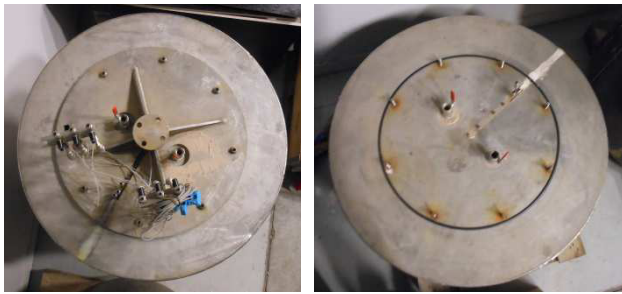


Figure 3. Bucket model with steel plate installed (left) and without steel plate (right).

2.3 Suction equipment

To simulate overburden pressure the sand is compressed by a suction system that create a depression inside the sand box.

Hermetic isolation is provided by a membrane made of non-porous latex rubber. The membrane has been cut so that can fit with the bucket model, it has a thickness that allow it to adapt to the sand surface. Four connection for suction pipes and one connection for surface pressure transducer are installed on the membrane.

Hermetic isolation along the perimeter of the sand box is provided by a groove where a circular rubber gasket is inserted. The membrane is stretched on the rubber gasket and the steel frame is placed on it and fixed with clamps (Figure 4).



Figure 4. Membrane fixed.



Figure 5. Suction Tank.

Suction tank (Figure 5) has a capacity of 320 liters, is provided of a barometer and is connected with the compressed air system of the laboratory. To activate the suction, both compressed air valve and the valve of the tank have to be opened. At this point suction starts and measures of pressures are sampled by Catman.

2.4 Loading and measuring systems.

Two hydraulic pistons are connected on the frame placed above the sand box: the installation piston and the loading piston (Figure 1).

Installation piston is used to run CPT tests and to install the bucket. It has a capacity of 200 kN and is actuated by a control, while speed has to be settled by the control panel in a range of 0.01-5 mm/s. Vertical displacement is measured by a displacement transducer connected to the transducers box, applied force is measured by a load cell. The signals are recorded by a computer with the program Catman.

Loading piston can apply a vertical force of 250 kN and has a maximum displacement range of 40 cm. Force or forced displacement for static and cyclic loading are applied with loading piston, controlled by the MOOG system whereby data are recorded and test are programmed. A wide range of options are available for cyclic loading in terms of frequencies and load modalities. Displacements are measured by two 125 mm displacement transducers, installed on a horizontal bar fixed at the side of the box, and connected to specific nuts installed at two opposite sides of the bucket (Figure 6). Displacement sensors are connected to the relative channels in the transducer box, signals are then elaborated and registered by MOOG system.



Figure 6. Displacement transducers WS10-1 and WS10-2 connected to the horizontal bar.

As shown in Figure 7, six pressure transducers are installed at different levels inside and outside the bucket. Installation valves and connection for pressure transducers are installed on top of the lid. Cable of pressure transducers are connected to the signal transducers box and through the signal amplifier MGCplus and Spider 8, the signal is elaborated by Catman.

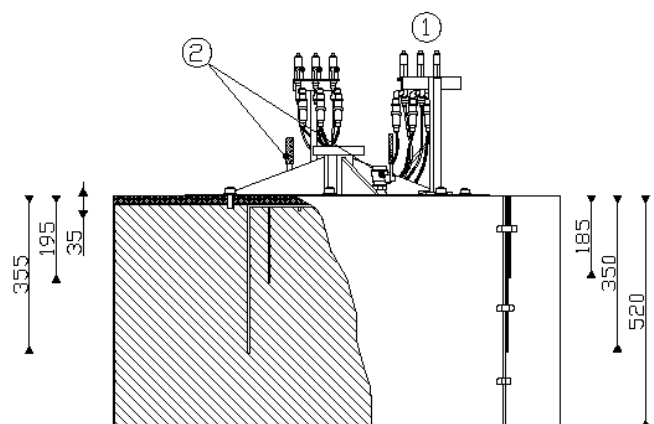


Figure 7. Section of bucket model. Distance of pressure transducers inside and outside the bucket are shown. Connection for pressure transducers (1) and installation valves (2).

A pressure sensor is placed outside and connected to MGCplus system, in order to have a measurement of ambient pressure.

3. SOIL DESCRIPTION.

Sand utilized is Aalborg University Sand No. 1. This sand is a graded sand from Sweden and the shapes of the largest grains are round, while the small grains have sharp edges. The main part of Baskarp Sand is quarts, but it also contains feldspar and biotit. Distribution of the grain size is shown in Figure 8 (Hedegaard & Borup 1993).

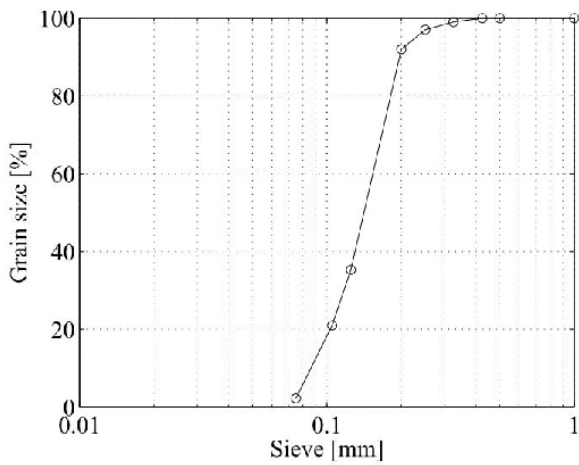


Figure 8. Grain distribution of Aalborg University Sand No. 1

Parameters of the soil have been estimated by Hedegaard & Borup (1993) are reported in Table 1. Other parameters such as friction angle ϕ , dilation angle ψ , relative density D_r , void ratio e , and effective unit weight of the sand γ' are inferred by empirical relations given in Ibsen et al. (2009).

50% quantile	d_{50}	0.14 mm
Uniformity coefficient	d_{60}/d_{10}	1.78
Specific grain density	d_s	2.64
Maximum void ratio	e_{max}	0.854
Minimum void ratio	e_{min}	0.549
Permeability	$K_{e=0.612}$	$6.89 \cdot 10^{-12} \text{ m}^2$

Table 1. parameters of Aalborg University Sand No. 1 (Sjelmo 2012), (Hedegaard & Borup 1993).

3.1 Soil preparation

To obtain homogeneity of the soil and so ensure comparability between tests, the procedure described in the following has been settled, based on previous experiences (Fisker, L.B., and Kromann. K. 2004).

First the groove along the perimeter of the sand box is cleaned by compress air and paper, then the rubber gasket is placed and aluminium frame is fixed by clamps. Being aware to match marks on the aluminium frame with marks on the sand box.

To loosen the sand, an upward gradient of 0.9 is applied opening gradually the inflow valve, ensuring to do not exceed the red line on the piezometer otherwise piping can occur. To avoid air infiltration during vibration, water is let to rise approximately 8 cm above the sand surface. To reach this level, the inflow valve is closed and additionally water has to be poured from the top, placing a small panel on the area of interest so as soil in the surface do not move.



Figure 9. Vibration starts inserting the rod vibrator in the hole marked in yellow.

A wooden panel with symmetrically distributed holes is placed on the box (Figure 9), then rod vibrator is systematically pushed and pulled in the sand, first in holes marked by a dot and then in holes without dot. A mark on the vibrator is made to ensure to reach a depth of 60 cm in case of M1 bucket or 110 cm in case of M2 bucket. During vibration it is important to keep the rod vibrator as perpendicular as possible and maintain a constant slow velocity in order to have a uniform vibration and allow the air to come out. After vibration the outflow valve is opened and water level is lowered till one centimeter above the sand surface, then the wooden plates are removed and the surface is first cleaned manually, then levelled using a specific shaped aluminium beam.

3.2 CPT tests

Cone penetration tests are carried out to have complete information about compaction and homogeneity of the soil.

CPT probe used is shown in Figure 10. It has a diameter of 15 mm, tip area of 176.7 mm, cone angle of 60° and penetration length of 120mm It is connected to the

installation pistons then force transducer is plugged in the signal transducer box. Afterwards four CPT tests in four different position are run, moving and fixing each time the installation piston in the corresponding position, each position is marked by the corresponding number on the inner side of the transverse IPE profile.



Figure 10. CPT probe.

The penetration velocity has to be settled on 5 mm/s, then the piston is activated and stopped at the sand surface. At this point Catman program is reset and then run registering data of the penetration resistance q_c , time and vertical displacement. The installing piston is activated until a depth of 110 mm, to help on this step, a yellow tag is attached on the probe.

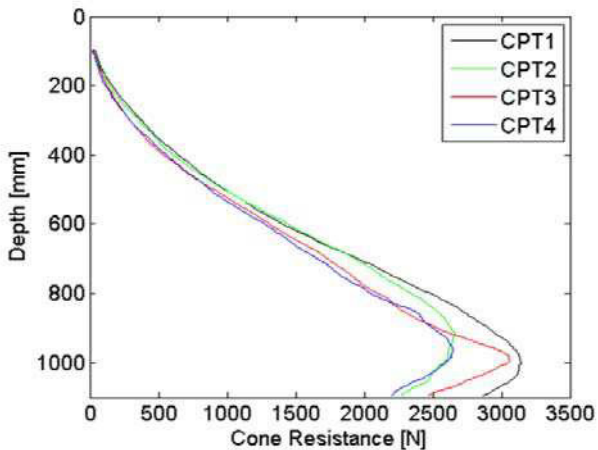


Figure 11. CPT test results for test n°5

In Figure 11 shows the typical results of cone penetration test made in the four positions of the test rig. Trend of the curves shows a cone resistance that uniformly increases with depth till a depth of approximately 600 mm. This is a satisfactory soil preparation for a M1 Bucket test, since depths of interest are from 0 to 500 mm.

Figure 12 shows the variation in relative density with respect to depth. Iterative process to calculate D_r is described in *Ibsen et al. (2009)*.

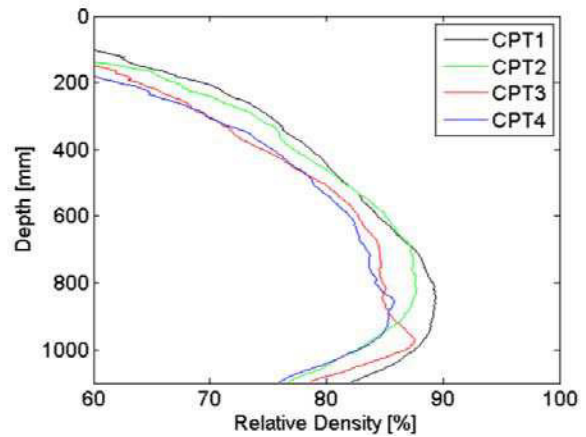


Figure 12. Relative density for test n°5.

4. TEST PROCEDURES.

In the following, steps on how to run tests are described. Soil preparation is common for both tests with and without membrane. Steps of installation are the same for both long and short bucket. Only differences are the longer time and greater preloading force required in the installation of long bucket M2.

4.1 Test without membrane

The water level is raised till 5-8 cm above the surface level, and so is kept while tests are run. The bucket is prepared first blowing out the sand from pipes of pressure transducers. Pipes are filled with water by immersing the bucket in a water box and, using suction equipment, water is sucked inside pipes (Figure 13). During this phase check that pipes are completely full of water and no bubble air are present.



Figure13. Bucket immersed in the water box.

The bucket is connected to the installation piston and speed is set on 0.2 mm/s. Before to activate the piston, installation

valves have to be opened and Catman run to register loading and displacement data. Despite the low speed, such installation does not reproduce all phenomena happening during the real installation. On the field installation suction is applied and a flow is created around the skirt, helping the penetration.

To ensure comparability between different tests, a preloading load of 70 KPa is reached before to close the two valves of the lid. An indicator of a good installation is water flowing out from the two valves of the lid, since no air is trapped between lid and soil.

Figure 14 is showing installation loading curve that is similar for all tests, since sand and sand properties like relative density and saturation are uniformed by soil preparation. In the first part of the curve it can be seen the increase of resistance due to skin friction of the sand adjacent to the caisson. When the lid touches the surface, the load is let to increase till 70 kN.

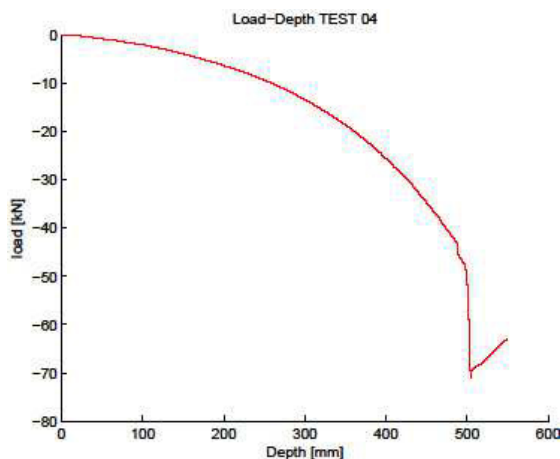


Figure 14. Installation load curve for static test.

Once installation has been completed, installation piston is disconnected and activated with an upward speed velocity of 0.2 mm/s, in order to limit disturbance to the installed bucket. Despite this precaution a slight bump of the lid of the bucket is unavoidable, this is due to the bending of the bucket lid happening during installation process.

Loading piston is positioned in the central position of the horizontal beam and fixed with 8 bolts. To connect the loading piston with the bucket, a light safety limit of the force has to be set in MOOG, so when the two parts start touching each other the system automatically stops, and the four bolts of the connection can be fixed.

Pressure sensors are connected to the signal transducers box. Data of pressures, load and displacement are registered by both MOOG and Catman.

4.2 Test with membrane

To simulate overburden pressure test with membrane have to be set. Overburden pressure is simulated in order to have a greater value of stress at the level of the lid. This allows simulating a bucket with longer skirt, and so applying a bigger scale. A drawback of suction is that also water is aspirated out of the sand box, so the sand layer is not fully saturated.

To start the test, first the bucket is prepared fixing the membrane under the steel plate of the bucket as shown in Figure 15. Preparation and installation of the bucket are then the same as described in section 3.1.



Figure 15. Membrane fixed under the lid.

After the bucket is penetrated into sand, the filter is laid on the sand and the membrane is outstretched so that overlay the rubber gasket placed on the perimeter. A metal ring is positioned and fixed with clamps. Installation piston is then removed and load piston is connected as indicated in the procedure of without membrane test.

Suction pipes are connected to the membrane and the suction system is activated. The pressure level is measured by Catman and, once reached the required value, has to be kept constant for at least 12 hours.

5. RESULTS PRESENTATION.

In the following is shown how results can be presented. A Matlab code has been created so that data can be elaborated and plotted. All tests presented are carried out with the bucket model M1 ($L/D=0.5$) numbers in Figure 16 are showing the corresponding position of pressure measurements.

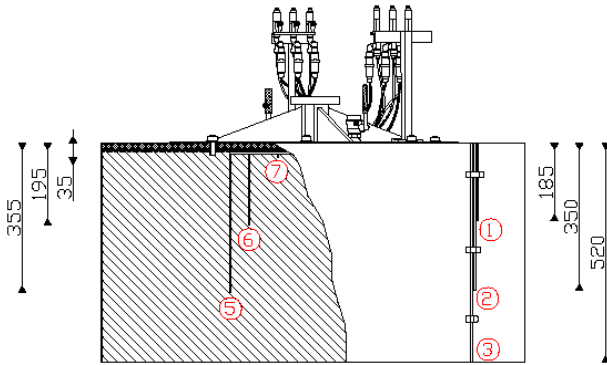


Figure 16. Position of pressure measurements.

5.1 Static test without suction

Figure 17 is shown the expected trend for a static load-displacement curve. In this case in MOOG it has been set up a vertical displacement of 60 mm that has to be reached in 3000 seconds. The load is suddenly increasing reaching a value of 7.8 kN, than is slightly decreasing till a value of 6.2 kN before to drop in correspondence of the end of the test.

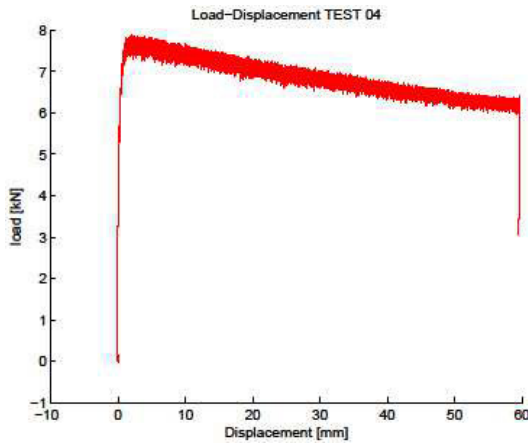


Figure 17. Load-Displacement curve for static test.

To show pressure measurements, it has been chosen to split the results in two graphs. In Figure 18 and Figure 19 measures respectively inside and outside the bucket model are shown. Measurement of atmospheric pressure given by “p6a” channel is shown in both graphs, this is made in order to have a reference point and allow a better comparison between results.

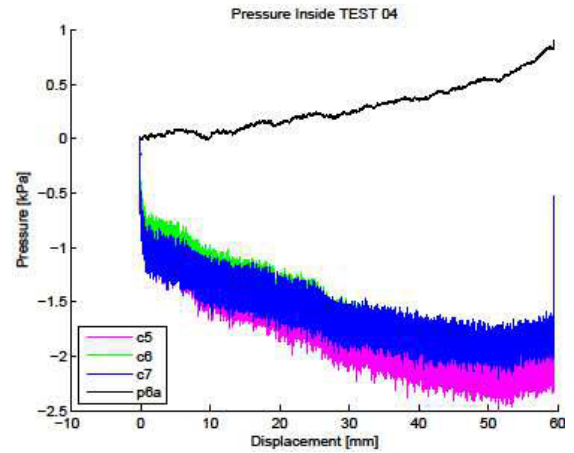


Figure 18. Pressure measurements inside the bucket.

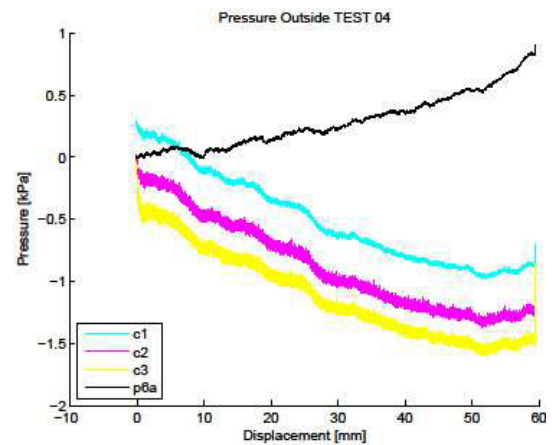


Figure 19. Pressure measurements outside the bucket.

5.2 Cyclic test without suction

Figure 20 shows a load-displacement curve for a cyclic test. Considering results of static test, for the cyclic test 40000 cycles has been settled with a frequency of 0.1 Hz and an amplitude of 50% of the static maximum load. Before of the cyclic load, the bucket is loaded with a static tensional load of 50% of the static maximum load, by “round ramp” mode.

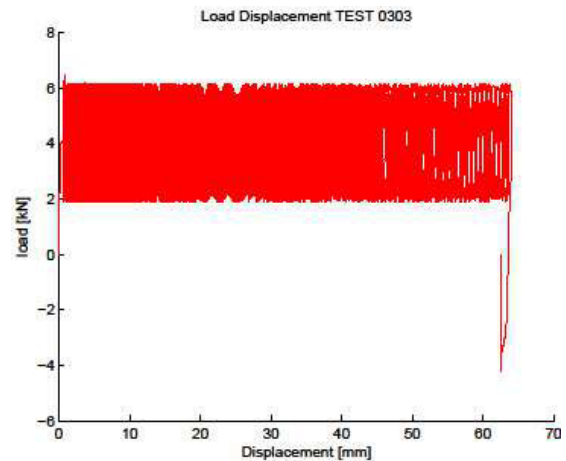


Figure 20. Load-Displacement curve for cyclic test.

Pressure results are presented in the same way as for the static test, as can be seen in *Figure 21* and *Figure 22*. Pressure measurements presents a wide fluctuation so, in order to have a more clear plots of results, a “reduced plotting” function has been used in the Matlab code.

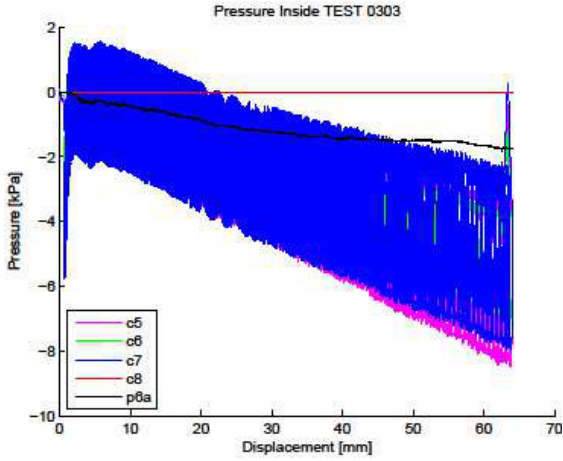


Figure 21. Pressure measurements inside the bucket.

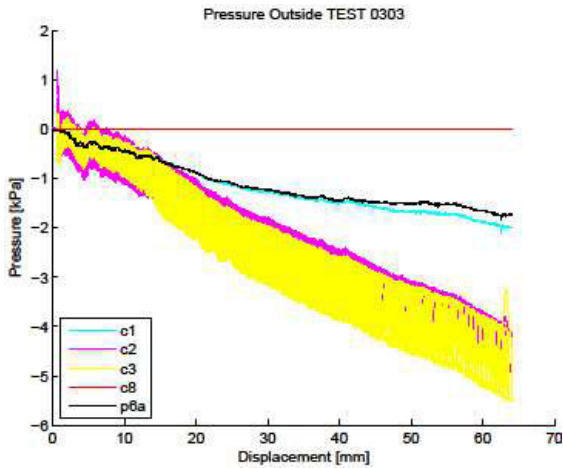


Figure 22. Pressure measurements outside the bucket.

6. VALIDATION OF RESULTS.

Methods presented in this work are divided in CPT based methods and beta-methods, based respectively on cone resistance and $\beta = K \tan \delta$. Effect of suction is not considered, since this phenomenon is not present in test used to validate results.

Methods to calculate pull-out resistance without considering passive suction are representing response of a totally drained behavior, where drainage conditions does not allow pore pressure to build up. In these methods only frictional resistance is taken into account.

To compare installation methods, the weight of the caisson is not considered, since piston used for installation has been

reset to zero value with the caisson connected. The skirt-soil friction angle δ is kept constant to a value of 30° , since this is the most suitable value for very dense sand in contact with steel, as confirmed in Table 2-1 in *Senders (2008)*.

Installation of a bucket foundation carried out by pushing, requires more force than installation where active suction is applied. The negative pressure, in non-cohesive soils, is helping installation creating a flow from outside to inside the caisson that, acting on friction resistance, results in a beneficial effect for skirt penetration.

In order to compare results, load and displacements are plotted in dimensionless form, respectively as $V/(D^3 \gamma)$ and h/D , according to *Kelly et al. (2006)*. In the following study, parameters are evaluated from responses of test 6, test 9, and test 11, carried out with overburden pressure of respectively 0kPa, 40kPa, and 20kPa.

6.1 Beta methods.

Installation beta methods (Houlsby et al. 2005a).

In *Houlsby et al. (2005a)*, it is reported a method to evaluate the pushing installation resistance of a suction caisson following the conventional pile design practice. The suction caisson is modelled as an open-ended pile, having the tip area equal to the thickness of the skirt. Installation resistance is evaluated as the sum of end-bearing resistance, friction outside the skirt and friction inside the skirt, as shown in the *Formula 1*.

$$V' = \frac{\gamma' h^2 (K \tan \delta) (\pi D_o)}{2} + \frac{\gamma' h^2 (K \tan \delta) (\pi D_i)}{2} + (\gamma' h N_q + \gamma' h N_\gamma) (\pi D t) \quad (1)$$

This method is un-conservative, as stated in *Houlsby (2005a)*, given that is not taking into account the enhancement given by friction to the vertical stress next to the skirt.

The increase of vertical stress with the depth considering enhancement given by skin friction, is calculated in *Houlsby (2005a)*, making equilibrium of vertical forces on a disc of soil adjacent to the skirt, where also soil-caisson frictional forces are taken into account. On the equilibrium of vertical forces inside the skirt, width of the disc is equal to the internal diameter, whereas outside the skirt, width of the disc is governed by parameter m . Therefore the whole internal plug and a constant section outside the skirt are affected by the enhancement in vertical stresses. *Formulae 2* and *3* are solutions of the equilibrium for, respectively, internal and external vertical forces.

$$\frac{d\sigma'_{vi}}{dz} = \gamma' + \frac{\sigma'_{vi}}{Z_i} \quad (2)$$

$$\frac{d\sigma'_{vo}}{dz} = \gamma' + \frac{\sigma'_{vo}}{Z_o} \quad (3)$$

Where

$$Z_i = \frac{D_i}{(4(K \tan \delta)_i)} \quad (4)$$

$$Z_o = \frac{D_o(m^2 - 1)}{(4(K \tan \delta)_o)} \quad (5)$$

If *Formula 6* is verified, end bearing stress is calculated with *Formula 7*

$$\sigma'_{vi} - \sigma'_{vo} < \frac{2tN_\gamma}{N_q} \quad (6)$$

$$\sigma'_{end} = \sigma'_{vo}N_q + \gamma' \left(t - \frac{2x^2}{t} \right) N_\gamma \quad (7)$$

Where

$$x = \frac{t}{2} + \frac{(\sigma'_{vo} - \sigma'_{vi})N_q}{4\gamma'N_\gamma} \quad (8)$$

If *Formula (9)* is verified, then $x = 0$ and the end bearing resistance is evaluated by *Formula (10)*.

$$\sigma'_{vi} - \sigma'_{vo} \geq \frac{2tN_\gamma}{N_q} \quad (9)$$

$$\sigma'_{end} = \sigma'_{vo}N_q + \gamma' t N_\gamma \quad (10)$$

In the method proposed by *Houlsby (2005a)*, the vertical load on the caisson for penetration to depth h is given by *Formula 11*.

$$\begin{aligned} V' = & \gamma' Z_o^2 \left(e^{\frac{h}{Z_o}} - 1 - \frac{h}{Z_o} \right) (K \tan \delta) (\pi D_o) \\ & + \gamma' Z_i^2 \left(e^{\frac{h}{Z_i}} - 1 - \frac{h}{Z_i} \right) (K \tan \delta) (\pi D_i) \\ & + \sigma'_{end} \end{aligned} \quad (11)$$

Pull-out beta methods (Houlsby et al. 2005b).

Methods presented in *Houlsby (2005b)*, are calculating pull-out friction resistance summing internal and external friction on the skirt. It is assumed that the soil immediately breaks the contact with the lid of the caisson, furthermore effective stresses along the bottom rim of the skirt are considered negligible.

Two methods are presented. The linear method is calculating the friction resistance summing internal and external friction following the conventional pile design practice (*Formula 12*).

$$V' = \frac{-\gamma' h^2 (K \tan \delta) (\pi D_o)}{2} + \frac{-\gamma' h^2 (K \tan \delta) (\pi D_i)}{2} \quad (12)$$

Second method is taking into account the reduction in vertical stress given by the friction further up the skirt (*Formula 13*). On the internal side of the skirt, all the plug is affected by stress reduction. On the outside of the skirt a parameter m is defining the zone of stress reduction. Therefore internal and external friction are calculated considering uniform stress, and the zone of vertical stress reduction is assumed constant along the skirt.

$$\begin{aligned} V' = & -\gamma' Z_o^2 y \left(\frac{h}{Z_o} \right) (K \tan \delta) (\pi D_o) \\ & - \gamma' Z_i^2 y \left(\frac{h}{Z_i} \right) (K \tan \delta) (\pi D_i) \end{aligned} \quad (13)$$

In both methods it has to be checked that the internal friction resistance does not exceed the weight of the soil plug inside the caisson, this condition is expressed by *Formula 14*.

$$\frac{\gamma' h \pi D_i^2}{4} > \int_0^h \sigma'_{vi} (K \tan \delta) (\pi D_i) dz \quad (14)$$

6.2 CPT-based methods.

DNV CPT-based installation method.

DNV presents a method to estimate the installation resistance of steel caisson based on the average cone resistance q_c . End-bearing resistance and friction resistance on the skirt, are related to q_c respectively by constants k_p and k_f , of which suggested ranges are listed in *Table 2*.

k_p		k_f	
Most probable	Highest expected	Most probable	Highest expected
0.3	0.6	0.001	0.003

Table 2. Parameters suggested by DNV.

Installation resistance is calculated summing friction forces and end-bearing resistance by *Formula 15*.

$$V_{in} = F_i + F_o + Q_{tip} \quad (15)$$

Where internal friction, external friction and end-bearing resistance are given respectively by *Formulae 16, 17, 18*.

$$F_i = A_{si}k_f \int_0^h q_c(z)dz \quad (16)$$

$$F_o = A_{so}k_f \int_0^h q_c(z)dz \quad (17)$$

$$Q_{tip} = A_{so}k_p q_c(z) \quad (18)$$

A_{si} and A_{so} are respectively the inner and outer caisson perimeter, calculated as $A_s = D\pi$ inserting D as inner or outer diameter depending on the case.

Senders (2008) CPT-based installation method.

Senders (2008) suggests to modify CPT-based method presented in *DNV* using a different k_p and evaluating k_f with *Formula 19*.

$$k_f = C * \left(1 - \left(\frac{D_i}{D_o}\right)^2\right)^{0.3} * \tan \delta \quad (19)$$

Where $C=0.21$ is a constant suggested by *Lehane et al. (2005)*.

k_p factor is taking into account differences in shape between the circular cone and the strip geometry of the caisson rim. Values of the shape factor s_q , giving the ratio between N_q for circular and strip footing, had been extrapolated and are showed in *Figure 23*, where are plotted with respect to the friction angle. In *Senders (2008)* it was noticed that s_q factor is in line with the range of k_p factor suggested by *DNV*, and s_q was therefore substituted to k_p in the calculation.

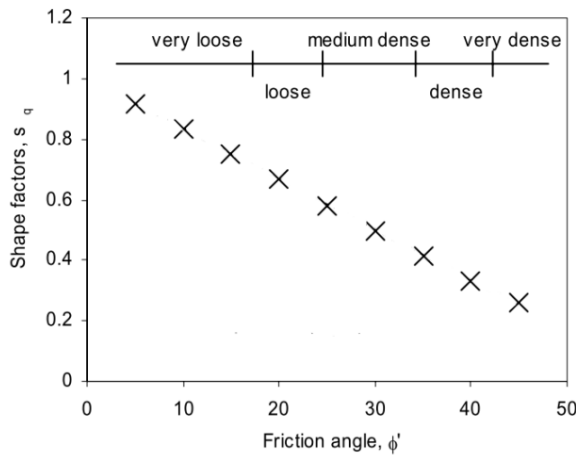


Figure 23. Theoretical shape factor (Randolph 2004).

In the present work it is chosen to use $k_p = s_q = 1 - 0.016\phi' = 0.1536$.

CUR pull-out CPT-based method.

Method suggested by *CUR* introduces a constant $k_f = 0.004$ *Senders (2008)* to evaluate the frictional pull-out resistance from q_c . Friction resistance in drained condition is calculated by *Formula 20*.

$$V_{out} = F_i + F_o \quad (20)$$

In the method suggested by *CUR*, internal and external friction are given respectively by *Formula 21* and *Formula 22*.

$$F_i = -A_{si}k_f \int_0^h q_c(z)dz \quad (21)$$

$$F_o = -A_{so}k_f \int_0^h q_c(z)dz \quad (22)$$

Senders CPT-based pull-out method.

Senders (2008) proposed a CPT based method where friction resistance is calculated following *CUR* procedure, but a different value of k_f is introduced (*Formula 23*). k_f from compressive capacity is corrected considering the ratio between tensile and compressive friction. This ratio was extrapolated from experimental results in centrifuge tests by *Senders (2008)*, as -0.375 , therefore is reducing pull-out friction resistance with respect to installation friction resistance. In the present work, the ratio between tensile and compressive friction is evaluated from back-calculation and experimental responses as -0.1652 , and is substituted to -0.375 in *Formula 23*.

$$k_f = -0.1652 C \left(1 - \left(\frac{D_i}{D_o}\right)^2\right)^{0.3} \tan \delta \quad (23)$$

6.3 Validation of CPT-based methods.

Validation of installation CPT-based methods.

In order to show how different value of k_f are affecting results of CPT-based methods, in Figure 24 are plotted responses keeping constant $k_p=0.3$, while k_f is varying on the range proposed in DNV (Table 2).

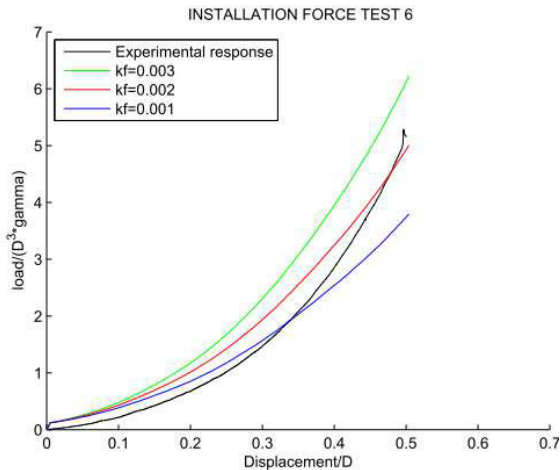


Figure 24. DNV method with constant $k_p=0.3$ while k_f is varying.

Figure 25 is showing the effect on the response varying k_p in the range suggested by DNV, and maintaining constant $k_f=0.002$. As can be noticed from Figure 24 and Figure 25, increase of the response is directly proportional to k_f and k_p .

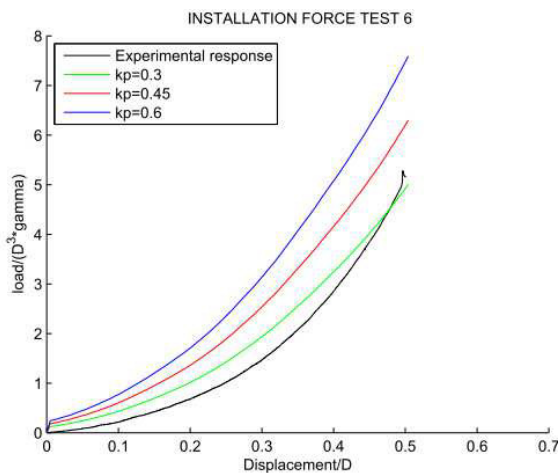


Figure 25. DNV method with constant $k_f=0.002$ while k_p is varying.

Parameters of method suggested by Senders (2008) are evaluated as $k_f=0.0032$ (Formula 19), and $k_p=0.1536$ (Figure 23). Best fit of parameters in DNV method is obtained with $k_f=0.002$ and $k_p=0.3$. Responses are shown in Figure 26.

Both CPT-based methods are giving a good approximation of the experimental response, as can be seen from Figure 26.

Peak of the experimental response is $4.92D^3\gamma'$, peaks in Senders (2008) and DNV methods are, respectively, $5.1D^3\gamma'$ and $5.0D^3\gamma'$. Method proposed by Senders (2008) has a better slope, since the response is lower at the beginning and more steep at the end of the installation, therefore is following the experimental trend.

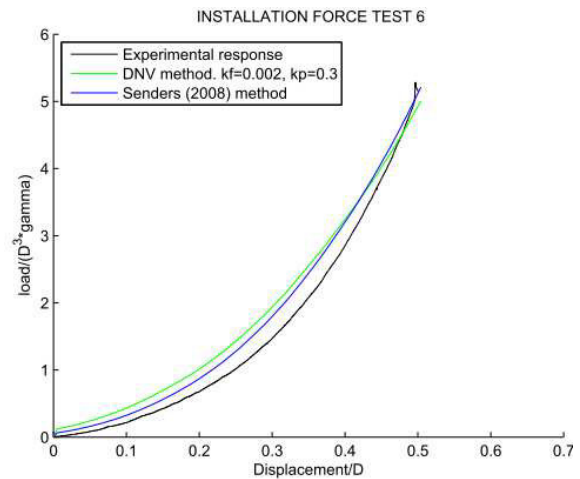


Figure 26. Comparison of DNV and Senders (2008) CPT-based methods.

Validation of pull-out CPT-based methods.

CPT-based method proposed in CUR is using a $k_f = 0.004$ (Senders 2008) that is heavily overestimating the experimental response, as shown in Figure 27. This is an expected results, inasmuch in CUR is presented also an installation method where is used a k_f greater than the one fitted in the previous section. Therefore methods presented in CUR are overestimating both installation and pull-out responses.

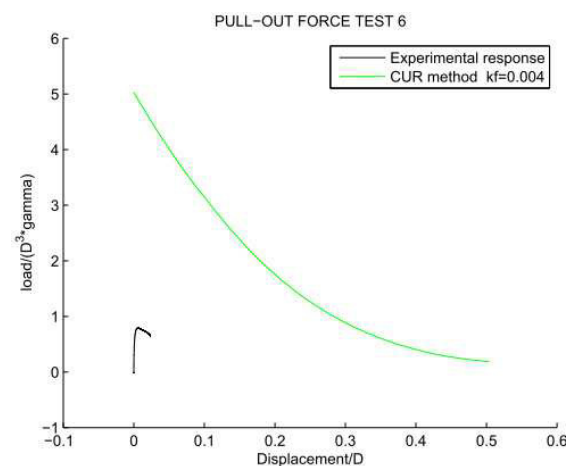


Figure 27 pull-out method presented in CUR, heavily overestimate the pull-out resistance.

It is chosen to find another value of k_f , based on the ratio between tensile and compressive friction 0.1652 and $k_f=0.003$, (Table 2). $k_f=0.1652*0.003=0.00049$ is obtained, and is giving a good approximation of the pull-out load for tests without overburden pressure. As can be seen in Figure 28, modified CUR method has a peak value of $0.785D^3\gamma'$ where the experimental result is $0.795D^3\gamma'$.

In test with 0kPa overburden pressure, CPT-based method proposed by Senders (2008) gives a slight overestimation of the pull-out resistance, due to the greater value of $k_f=0.00053$. As shown in Figure 28, Senders (2008) method reaches a peak value of $0.832D^3\gamma'$. This result is slightly un-conservative but, since the method does not need any fitting of parameters, method presented in Senders (2008) is considered the most reliable CPT-based method to evaluate pull-out resistance.

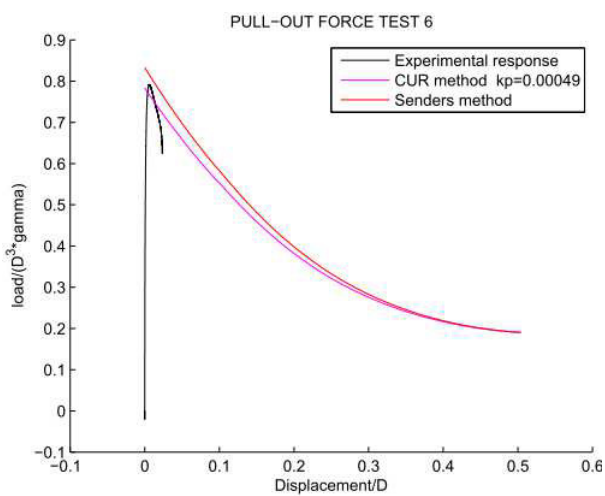


Figure 28 CPT-based method for test without overburden pressure.

In test where overburden pressure is applied, values of cone resistance are evaluated only before of the installation phase. After the application of overburden pressure, q_c is varying and at this stage, is not possible to carry out the CPT test. Therefore k_f values for test where overburden pressure is applied are fitted in formulae where q_c is measured without overburden pressure. In test where 20kPa and 40kPa of overburden pressure are applied, k_f are evaluated as, respectively, 4.5 and 5.7 times the k_f with zero overburden pressure. Function is fitted in order to evaluate k_f with different overburden pressures (Figure 29).

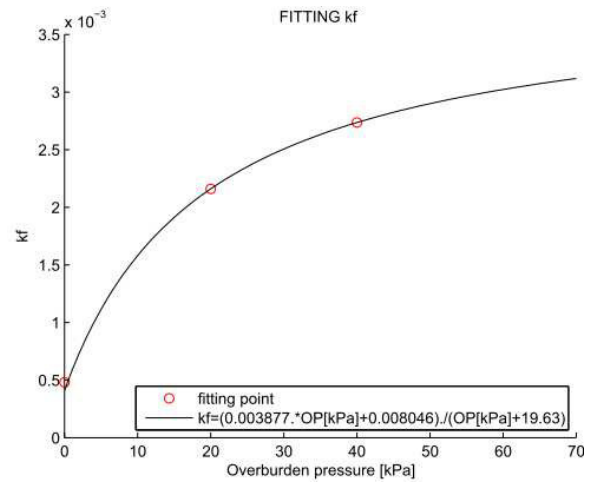


Figure 29 Function relating k_f and overburden pressure.

In Figure 30 and Figure 31 experimental responses are compared with methods results where k_f is evaluated following the curve in Figure 29. Methods are not applied properly, since as previously mentioned, q_c response is not measured after the application of overburden pressure. Therefore k_f approximation in Figure 29 has to be intended as an adaptation of CPT-based methods to the experimental apparatus of Aalborg University, not suitable for a more general application. Results in Figure 30 and Figure 31 are showing that CUR and Senders (2008) methods are respectively underestimating and overestimating the response. Therefore the same trend of zero overburden pressure response is maintained.

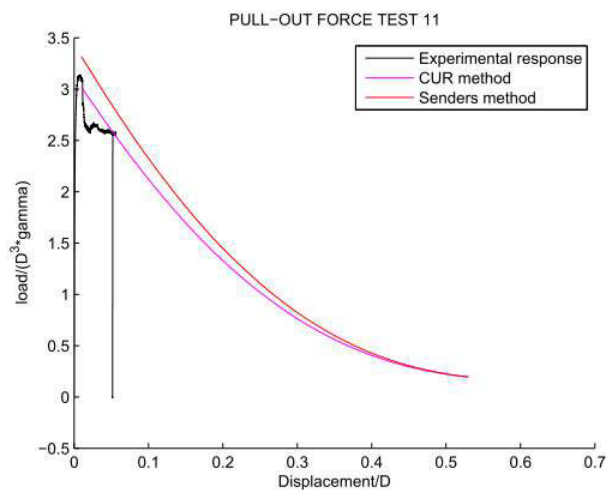


Figure 30 CPT-based methods for 20kPa overburden pressure.

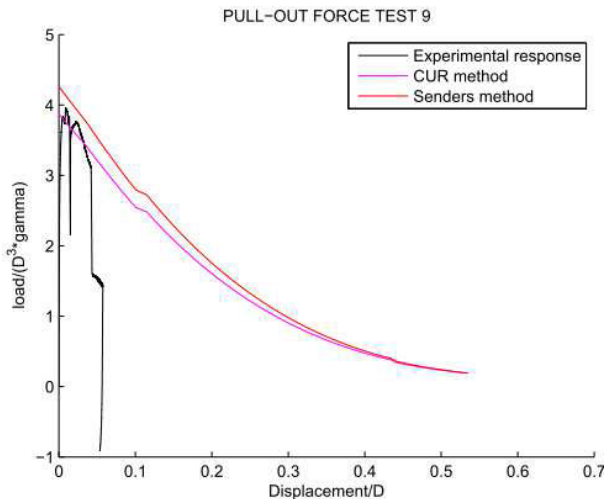


Figure 31 CPT-based methods for 40kPa overburden pressure.

6.4 Validation of beta methods.

Beta methods cannot be used for tests where overburden pressure is applied, since parameters of the soil are unknown. Therefore beta methods are validated only for test where overburden pressure is not present.

Validation of pull-out beta methods.

To verify beta methods proposed by *Houlsby et al. (2005b)*, first the coefficient of lateral earth pressure K is fitted in the linear method. K is the only unknown, and the linear method is expected to overestimate the pull-out resistance, since is ignoring the reduction of the stress given by skin friction.

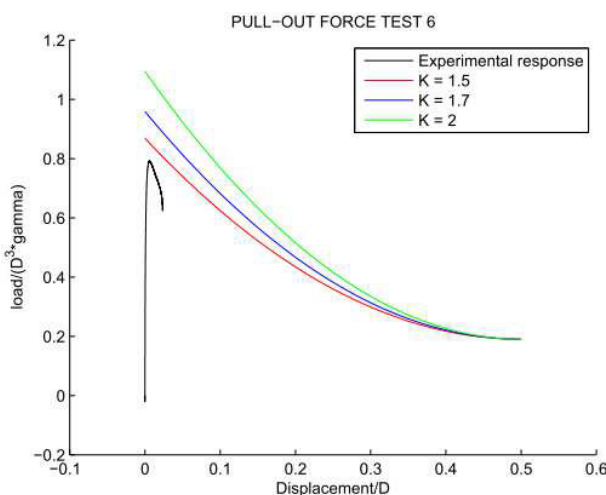


Figure 32 linear method response varying K .

All three responses plotted in *Figure 32* are overestimating the experimental response. Given that is not known how much the linear method should overestimate the experimental

response, in order to estimate K it is analyzed the sensitivity of the method proposed by *Houlsby et al.(2005b)* with respect to the variation of parameter m .

In *Figure 33* are shown responses obtained maintaining constant $K=1.5$ and varying the parameter m . Analyzing *Figure 33* it can be seen that increasing m , the reduction in vertical stresses decreases. This means that increasing the volume where upward skin friction is interacting with vertical stress, brings to a smaller total decrease of vertical stress. As can be seen the improvement of the response is higher from $m=1.5$ to $m=2$ with respect to the improvement obtained from $m=2$ to $m=3$, despite Δm is higher in the latter case. This trend is maintained also for higher values of m , and increasing the parameter m convergence with $K=1.5$ is not possible.

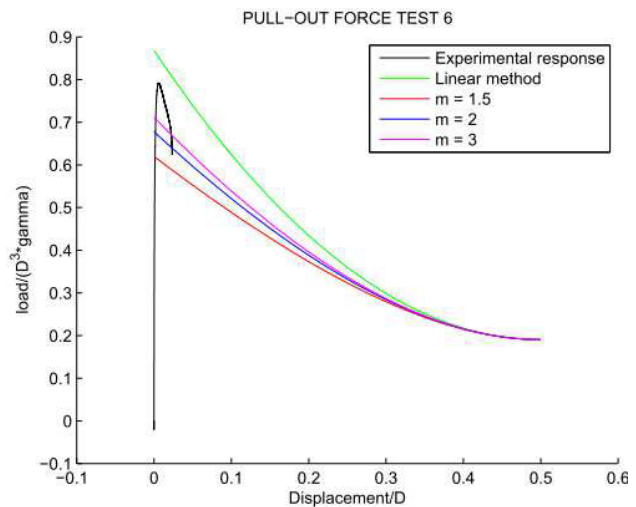


Figure 33 *Houlsby et al. (2005b)* method response, varying m maintaining constant $K=1.5$.

Same considerations made for *Figure 33* can be made for *Figure 34*, where method suggested by *Houlsby et al.(2005b)* is implemented maintaining constant $K=1.7$ and varying m .

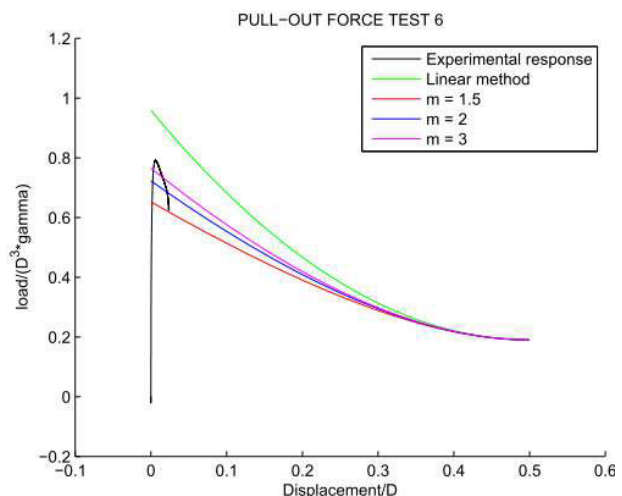


Figure 34 *Houlsby et al. (2005b)* method response, varying m maintaining constant $K=1.7$.

It is chosen to implement the second method maintaining a constant value of $K=2$, and varying the coefficient m in order to find the best fit, as shown in Figure 35.

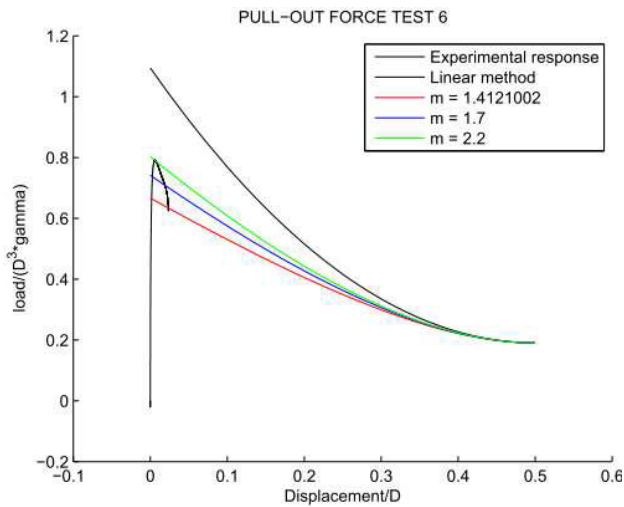


Figure 35 Housby et al. (2005b) method response, varying m maintaining constant $K=2$.

Referring to Figure 35, it is assumed that $m=2.2$ is a suitable value to implement this beta method.

In Figure 36 beta methods are plotted with constant $K=2$ and $m=2.2$, giving the best fit. Housby et al. (2005b) method gives a good approximation with a peak value of $0.8D^3\gamma'$, where the experimental response is $0.79D^3\gamma'$. Linear method reaches a value of $1.1D^3\gamma'$ overestimating the experimental response of $0.3D^3\gamma'$.

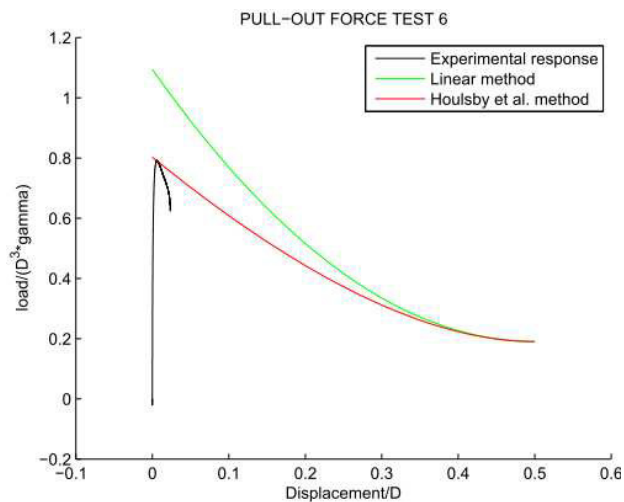


Figure 36 Comparison between the two beta-methods considered, constant used are $m=2.2$ and $K=2$.

It is considered of interest fitting K value when external and internal reduction of vertical stress is symmetrical, therefore with $m=1.4121002$. The response is shown in Figure 37.

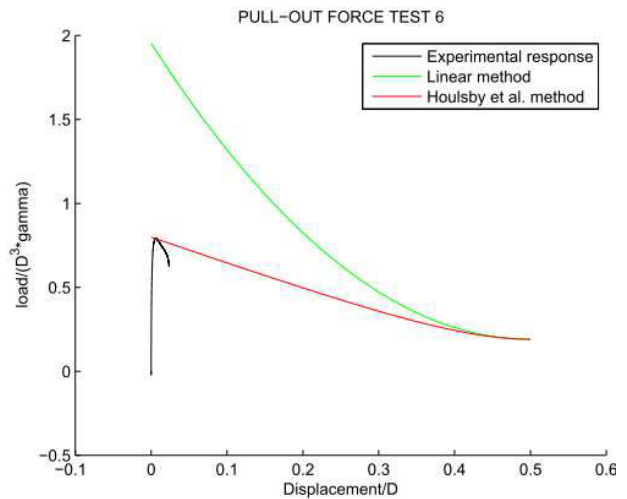


Figure 37 beta method responses, constant used are $m=1.4121002$ and $K=3.9$, reproducing a symmetrical distribution of vertical stress.

Fitted value of $K=3.9$ is considered too high for the examined case. Therefore it can be argued that, following the presented method, a symmetrical distribution of forces is not plausible, and frictional forces are affecting vertical stress in a heavily way on the inside of the skirt.

Validation of installation beta methods.

Installation beta methods are heavily affected on how end bearing factors N_q and N_γ are evaluated.

Larsen (2008) presented formulae to evaluate N_q and N_γ parameters for circular rough foundation. Convergence with these parameters is not possible, as can be seen from Figure 38, where is shown the response obtained with $K=0.8$ and $m=2$.

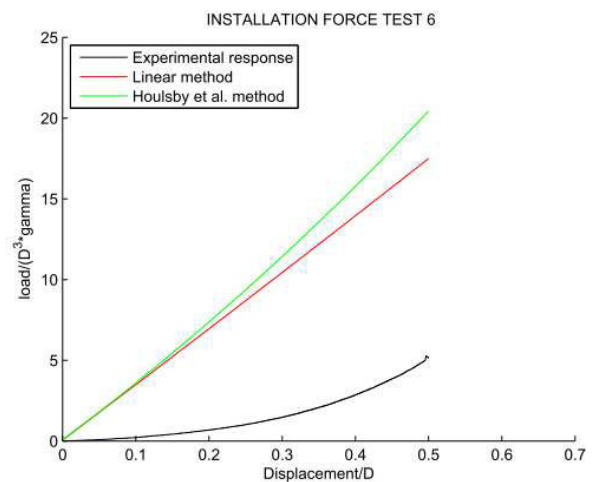


Figure 38. Beta methods implemented with N_q and N_γ from Larsen (2008). $K=0.8$ and $m=2$.

As can be seen in *Figure 38*, the linear method is heavily overestimating the experimental response, and, consequently, also *Houlsby et al. (2005a)* method.

It has been chosen to use $N_q = e^{\pi \tan \phi} \tan^2(45 + \phi/2)$ evaluated from *Prandtl (1920)*, and $N_\gamma = 1/4((N_q - 1) \cos \phi)^{1/2}$ according to *DS 415 (1998)*. Response evaluated with these factors is more realistic as can be seen in *Figure 39*, since is giving a lower end bearing resistance.

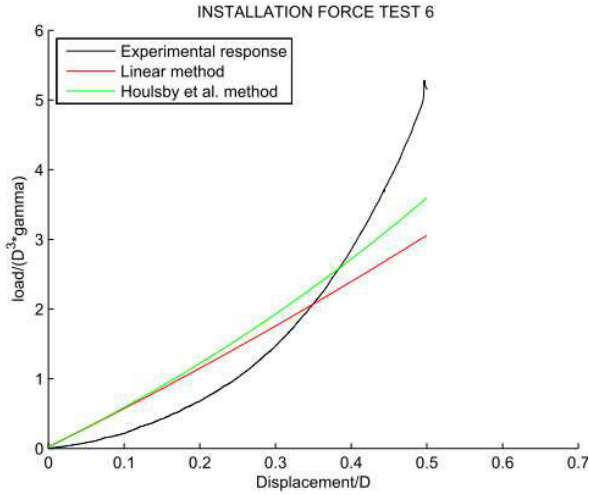


Figure 39. Beta methods implemented with N_q and N_γ according to Prandtl (1920) and DS 415 (1998). $K=0.8$ and $m=2$.

Method proposed by *Houlsby et al. (2005a)* is dependent on parameters m and K . The parameter m is defining the area affected by friction on the outside of the caisson. This area is an annulus, with internal diameter equal to D_o and external diameter equal to $D_m = D_o * m$, as shown in *Figure 40*. Inside the skirt, the whole area is considered affected by stress enhancement, and is identified as “internal area” in *Figure 40*.

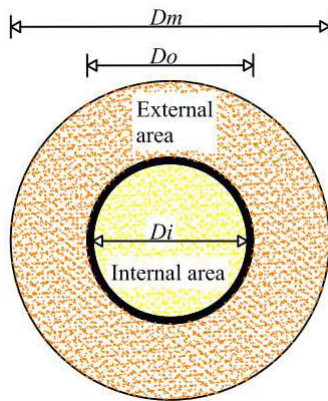


Figure 40. Horizontal section of a suction caisson installed in sand. Internal and external areas where stress are affected by friction enhancement are highlighted.

In *Houlsby (2005a)* it is mentioned that for all likely combination of parameters $\sigma'_{vi} \geq \sigma'_{vo}$. It has been noticed

that if this condition is satisfied, method proposed by *Houlsby et al. (2005a)* can always been applied.

Considering that the friction force is equal on both sides of the skirt, the enhancement of stress induced by this friction load is larger if the corresponding area is smaller. Therefore the external area has to be greater than the internal area in order to satisfy the condition $\sigma'_{vi} \geq \sigma'_{vo}$. This consideration brings to a limitation of the parameter m , given by *Formula 24*.

$$m \geq \sqrt{\frac{D_o^2 + D_i^2}{D_o^2}} \quad (24)$$

Since vertical stress inside and outside the caisson can differ in magnitude, distribution of stresses at the tip of the skirt can be not symmetrical, and depends on parameter x , (*Formula 8*), as shown in *Figure 41* (*Houlsby 2005a*).

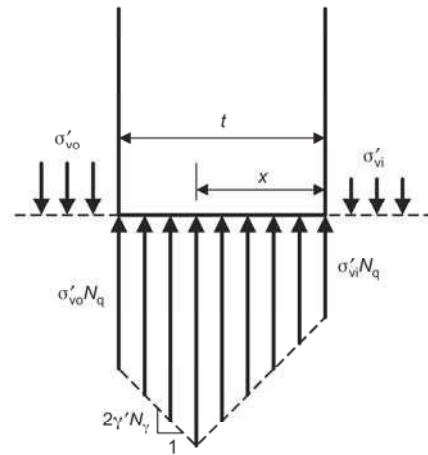


Figure 41. Definition of stress distribution on caisson tip on the basis of method proposed by Houlsby (2005a). (Houlsby 2005a).

Parameter x defines a length that cannot be neither greater than t nor smaller than zero, as can be deduced from *Figure 41* (*Houlsby 2005a*).

Condition $x \geq 0$ is taken into account in the method proposed in *Houlsby et al (2005a)* by means of *Formula 6* and *Formula 9*. These conditions are considered too strict, since from *Formula 8* it is obtained that $x > 0$ is verified also by condition in *Formula 25*.

$$\sigma'_{vi} - \sigma'_{vo} < \frac{2\gamma' N_\gamma t}{N_q} \quad x > 0 \quad (25)$$

Term on the right side of *Formula 25* is greater with respect to term on the right side of *Formula 6*, therefore *Formula 25* gives a less strict condition.

Beta method presented in *Houlsby et al (2005a)* does not give any specific restriction for $x \leq t$, this condition is satisfied

with good approximation if $\sigma'_{vi} \geq \sigma'_{vo}$. Therefore condition of parameter m given by *Formula 24* is used in this work. A less strict and more precise condition is given by *Formula 26*.

$$\sigma'_{vi} - \sigma'_{vo} \geq -\frac{2\gamma'N_{\gamma}t}{N_q} \quad x \leq t \quad (26)$$

As can be noticed from the discussion above, end bearing resistance calculated by means of *Formula 7* is restricted for a relatively small magnitudes of $\Delta\sigma'_v$, with values in a range of $\pm \frac{2\gamma'N_{\gamma}t}{N_q}$.

In the present work, condition given in *Formula 6* is substituted by less strict condition given in *Formula 25*.

From *Formula 24* it is evaluated the limit value of parameter $m=1.4121002$. Response evaluated with a value of $K=0.8$ suggested by *Senders (2008)*, is shown in *Figure 42*.

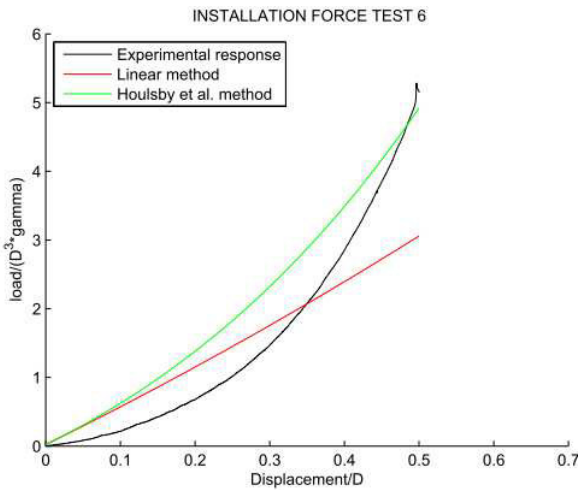


Figure 42. Beta methods, $K=0.8$ $m=1.4121002$.

Response of *Houlsby et al (2005a)* method shown in *Figure 42* gives a peak value of $4.91D^3\gamma'$, where the experimental response is $4.92D^3\gamma'$ therefore the estimated response can be considered precise. Linear method has a peak value of $3.1D^3\gamma'$ underestimating the experimental response as expected.

When the end bearing resistance is evaluated using the limit value of m , force distribution at the tip of the caisson (*Figure 41*) is symmetrical, since $x=t/2$. Seeing considerations made in the previous section for *Figure 37*, symmetrical distribution of vertical stress is not considered suitable for this method, therefore fitting showed in *Figure 42* is not considered satisfying.

It is chosen to adopt $K=2$, evaluated from pull-out beta methods. Responses where $K=2$ is maintained constant and parameter m is varying are plotted in *Figure 43*.

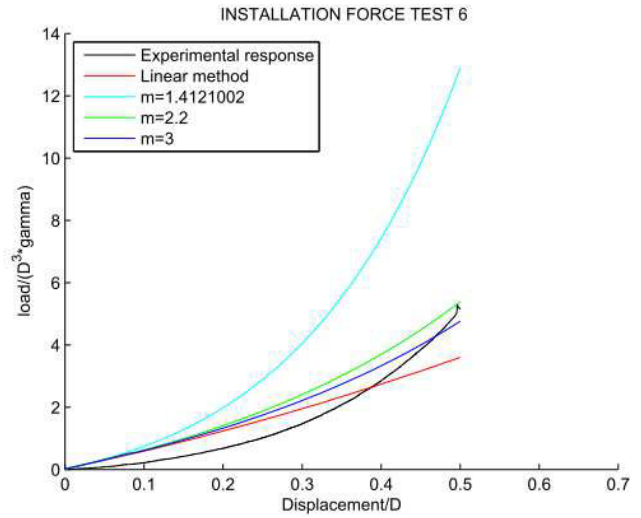


Figure 43. Beta methods responses maintaining constant $K=2$ and varying parameter m .

As can be seen in *Figure 43*, limit value of $m=1.4121002$, representing a symmetrical distribution of enhanced stress, is heavily overestimating the experimental response with a peak value of $12.89D^3\gamma'$. Responses obtained using $m=2.2$ and $m=3$ are giving respectively peak values of $5.4D^3\gamma'$ and $4.71D^3\gamma'$, where the experimental response is $4.92D^3\gamma'$. Result obtained with $m=2.2$ is considered acceptable, since is overestimating the experimental response, therefore is giving a safe approximation of the installation force.

A more precise fitting, shows that response evaluated with $K=2$ and $m=2.46$ gives a better approximation of the experimental result, since reaches a peak value of $5.0D^3\gamma'$, as can be seen in *Figure 44*.

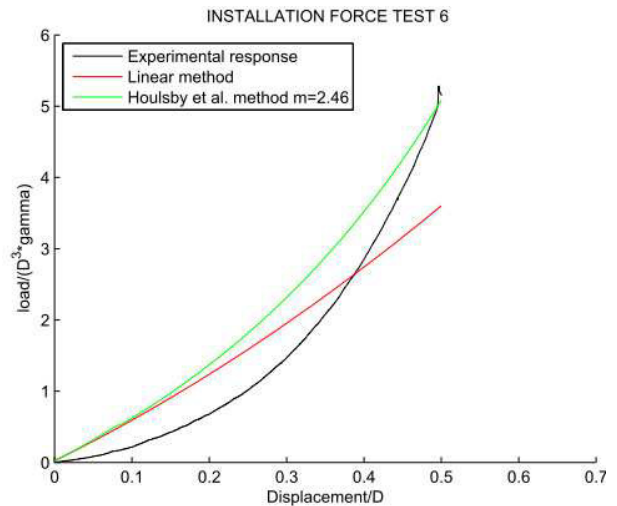


Figure 44. Beta methods, $K=2$, $m=2.46$.

Despite the good fitting shown in *Figure 44*, combination of parameters $m=2.2$ and $K=2$ is considered the most suitable, since is giving good approximation also in the pull-out beta method proposed by *Houlsby et al. (2005b)*.

7. CONCLUSIONS.

This article presents a testing rig of Aalborg University, and the procedure followed to carry out tests. Responses obtained are considered of high reliability, given the low scaling factor adopted ($1:10$) and the standardized procedure followed in each test.

The possibility to apply overburden pressure allows examining a wide range of skirt length. This allows extending the possibility of study to configurations otherwise not reachable.

Methods to evaluate pull-out and installation forces are validated, relying on responses obtained from tests described. More tests are needed in order to reach a better definition of parameters on which methods are based.

Since in installation measurements is not well defined where the lid makes contact with soil, an approximation on this value has been done. It is believed that more precise data can be obtained installing for a depth of 50cm the bucket model $M2$ ($L/D=1$). Following this expedient ensures that only frictional forces and end-bearing resistance at the tip of the caisson are present, therefore better parameters can be obtained.

On this article it is assumed that, for beta methods presented in *Houlsby et al (2005a; 2005b)*, $m=2.2$ is a suitable value. More precise evaluation of this parameter can be made running CPT tests also after installation and pull-out test. These CPT tests should be carried out at different distances from the outside of the skirt. Comparing responses of CPT test carried out at different stages, can give a better definition of the volume of sand affected by skin friction.

Given that beta methods to evaluate pull-out and installation resistance presented in *Houlsby et al (2005a; 2005b)* have been elaborated making approximations, also the parameter $K=2$ found in this work is affected by these approximations. On the inside of the caisson it is assumed that all the soil is affected by skin friction in the same manner, overestimating the enhancement/reduction of vertical stress. Therefore have a symmetrical distribution of the stress as shown in *Figure 37*, means to overestimate/underestimate vertical stress also outside the caisson. Parameter $m=2.2$ has the physical meaning of a diameter $D_m=2.2\text{m}$ that is affected by skin friction on the outside of the caisson. $D_m=2.2\text{m}$ is clearly an unlikely value, obtained because the effect of the friction on the outside of the caisson has to be underestimated in order to compensate the overestimation of the same effect on the inside of the skirt. A more precise beta method to evaluate installation force is presented in *Houlsby et al (2005a)*. This method is an improvement of beta methods presented in this work, since is defining a stress enhancement that increases with the depth. Despite a better approximation can be obtained, the improved method has some restrictions, and cannot be applied to a bucket with $L/D=1$. Therefore methods presented in this article has been considered more suitable to study the examined cases.

REFERENCES.

- Byrne, L.B. and Houlsby, G.T. (2003). "Foundation for offshore wind turbines", *Phil. Trans. of the Royal Society of London, Series A* 361, 2909-2300.
- CUR (2001) 2001-8; Bearing capacity of steel pipe piles, Centre for Civil Engineering Research and Codes.
- DNV (1992) Classification notes No 30.4, Hovik, Det Norske Veritas.
- DS 415 (1998) Norm for fundering (Code of Practice for foundation engineering), 4th. edition, Danish standard Copenhagen, In Danish.
- Fisker, L.B., and Kromann, K. (2004). "Cyklisk Belastning af Bøttefundament i Tryktank", Speciale ved Aalborg University.
- Houlsby, G.T. and Byrne, B.W. (2005a). Design procedures for installation of suction caissons in sand. *Proceedings of the ICE, Geotechnical Engineering* 158, No. 3, 135-144.
- Houlsby, G. T., Kelly, R. B. & Byrne, B. W. (2005b) The tensile capacity of suction caissons in sand under rapid loading. *Proc. International Symposium on Frontiers in Offshore Geotechnics (ISFOG)*. Perth, Australia, Taylor & Francis Group.
- Houlsby, G.T., Ibsen, L.B., and Byrne, B.W.(2005c) "Suction caisson for wind turbines" Department of Civil Engineering, Aalborg University Denmark, Department of Engineering Science Oxford University UK.
- Hedegaard, J. and Borup, M. (1993). "Data Report Baskarp Sand No 15", Division of Geotechnical and Foundation Engineering, Aalborg University.
- Ibsen L.B., Hanson, M Hjort, T. and Taarup, M. (2009) "MC-Parameter Calibration for Baskarp Sand No. 15" DCE Technical Report No.62. (ISSN 1901-726X), Aalborg University, Department of Civil Engineering, Aalborg, Denmark.
- Larsen K.A. (2008), *Static Behaviour of Bucket Foundations*, Ph.D. Thesis, Aalborg University, Department of Civil Engineering Division of Water & Soil. Aalborg, Denmark.
- Lehane, B. A., Schneider, J. A. & Xu, X. (2005) The UWA-05 method for prediction of axial capacity of driven piles in sand. *Proc. International Symposium 'Frontiers in Offshore Geotechnics'*. Perth, Australia, Taylor & Francis Group.
- Kelly, R. B., Houlsby, G. T. & Byrne, B. W. (2006). A comparison of field and laboratory tests of caisson

foundations in sand and clay. *Getotechnique*, 56, No. 9, 617–626.

Prandtl L. (1920) Über die Härte plastischer Körper, *Nachr. D. Ges.D.Wiss*, Göttingen 1920.

Randolph, M.F., Jamiolkowski, M. B. & Zdravkovic, L. (2004) Load carrying capacity of foundations. *Proc. Skempton Memorial Conf.* London.

Senders, M., (2008) Suction Caissons in Sand As Tripod Foundations for Offshore Wind Turbines, Ph.D. Thesis, University of Western Australia.

Sjelmo, Å. (2012) “Soil-Structure Interaction in Cohesionless Soils due to Monotonic Loading”, MSc. Student Report, Department of Civil Engineering, Aalborg University.

Sørensen, S. P. H., M. Møller, K. T., Augustsen A. H. Brødbæk, and L.B. Ibsen, (2009). Evaluation of Load-Displacement Relationships for Non-Slender Monopiles in Sand. DCE Technical Report No. 79. (ISSN 1901-726X), Aalborg: Aalborg University, Civil Engineering Department.

Digital Appendix

Digital appendix includes the following folders:

- “*InstallationMethods*”, containing four functions where are implemented four installation methods presented in section 6 of “*Laboratory Setup for Vertically loaded Suction Caisson Foundation in Sand and Validation of Responses*” and a respective main file to run.
- “*PullOutMethods*”, containing functions where are implemented four pull-out methods presented in section 6 of “*Laboratory Setup for Vertically loaded Suction Caisson Foundation in Sand and Validation of Responses*” and a respective main file to run.
- “*FittingKfCPTMethods*” containing a function on which Figure 29 of “*Laboratory Setup for Vertically loaded Suction Caisson Foundation in Sand and Validation of Responses*” is fitted.